*MRS Communications (2013)*, *3*, 13–29
© Materials Research Society, 2013
doi:10.1557/mrc.2013.9

MRS Communications

Prospective Articles

# Hairy nanoparticle assemblies as one-component functional polymer nanocomposites: opportunities and challenges

**Nikhil J. Fernandes,** School of Applied and Engineering Physics, Cornell University, Ithaca, New York 14853
**Hilmar Koerner,** Air Force Research Laboratory, Wright-Patterson Air Force Base, Ohio 45433
**Emmanuel P. Giannelis,** Department of Materials Science and Engineering, Cornell University, Ithaca, New York 14853
**Richard A. Vaia,** Air Force Research Laboratory, Wright-Patterson Air Force Base, Ohio 45433
Address all correspondence to Richard A. Vaia at **richard.vaia@wpafb.af.mil**

(Received 6 January 2013; accepted 27 February 2013)

## Abstract

Over the past three decades, the combination of inorganic-nanoparticles and organic-polymers has led to a wide variety of advanced materials, including polymer nanocomposites (PNCs). Recently, synthetic innovations for attaching polymers to nanoparticles to create "hairy nanoparticles" (HNPs) has expanded opportunities in this field. In addition to nanoparticle compatibilization for traditional particle–matrix blending, neat-HNPs afford one-component hybrids, both in composition and properties, which avoids issues of mixing that plague traditional PNCs. Continuous improvements in purity, scalability, and theoretical foundations of structure–performance relationships are critical to achieving design control of neat-HNPs necessary for future applications, ranging from optical, energy, and sensor devices to lubricants, green-bodies, and structures.

## Introduction

Over the last several decades there has been widespread appreciation of the potential of nanoparticle-filled polymer composites with very small added volumes of fillers, particularly in reference to their thermal, barrier, mechanical, and electrical performance.[1–5] These properties have been found to be very strongly dependent on the dispersion characteristics of nanoparticles in the polymeric matrix,[4–7] thus bringing the issue of structure control to the forefront. While this structure control can be achieved by carefully controlled processing techniques (such as blending conditions,[8] or external stimuli such as magnetic and electrical fields during synthesis)[7] scalability and reliability would be greatly improved if the desired structure and dispersion were intrinsically stable properties of the material itself. The use of polymeric shells grafted to nanoparticles, originally as a method of colloidal stabilization (van der Waarden reported the use of grafted polymers to stabilize colloids as early as 1950)[9–11] is now widely exploited to enhance dispersion and mixing of the particles into an organic solvent or matrix by creating a compatibilizing layer between the inorganic nanoparticles and the organic matrix.[12,13] These "hairy" nanoparticles (HNPs) consist of a central core surrounded by an organic (typically polymeric) corona. The dispersion of these HNPs into a matrix has been shown strongly dependent on graft density, and the nature and degree of polymerization of the corona and matrix.[14,15]

A subset of nanocomposites are based on self-suspended HNPs (i.e. HNP systems that are void of solvents or extra polymer matrix). Self-suspended HNPs offer significant advantages over traditional filled nanocomposites. Since the organic component is tethered to the particle, demixing is impossible without breaking the linkage. This architecture overcomes the "mixing problem" associated with incorporating nanoparticles into polymers,[8] producing exceptionally stable and uniform dispersions. Furthermore, HNPs can combine the properties associated with the inorganic core (band gaps, dielectric properties, and superparamagnetism, to name just a few) with the processibility and mechanical properties of the organic component in one simple platform. In this perspective, we examine the recently demonstrated potential of HNP assemblies and consider both the challenges involved in modeling and synthesizing these systems, and the opportunities that these systems offer for advanced materials of the future.

We limit the scope of our discussion to the following criteria [Fig. 1(a)]: (i) the nanoparticle core has dimensions between 1 and 200 nm; (ii) the nanoparticle core is rigid (either inorganic or macromolecular) and there is a well-defined interface between the core and the corona; (iii) the corona consists of noncrosslinked organic molecules tethered strongly (via a covalent or ionic bond) at a single point to the core at the interface; (iv) the entire organic fraction is strongly associated with the core—there is no separate solvent or matrix component [Fig. 1(b)]. These criteria distinguish the HNPs considered here from polymer-stabilized colloids (which can range to one micron in size,[16] and are dispersed in a solvent), star polymers (which do not have a well-defined interface between the



https://doi.org/10.1557/mrc.2013.9 Published online by Cambridge University Press

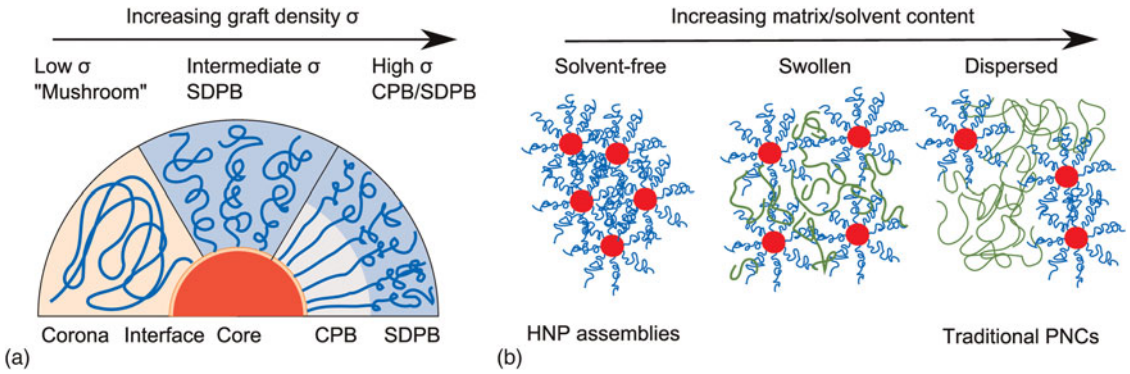



**Figure 1.** (a) Structure of hairy nanoparticles (HNPs) at different graft densities. At grafting densities, $\sigma$, of less than $Rg^{-2}$, the corona is in a loosely coiled "mushroom" conformation. As the grafting density increases, the chains are forced to extend first into a semidilute polymer brush (SDPB), and then into a concentrated polymer brush (CPB) conformation. In contrast to flat surfaces, particle curvature implies that the area per chain increases with distance from the surface, and thus the outer ends of the chain are less crowded and may transition to the SDPB regime if long enough. (b) The mesoscopic continuum from pure HNP assemblies (left) where the only swelling of the corona is by the corona of neighboring particles, to traditional polymer nanocomposites (PNCs) (right) where the particles are dispersed or suspended in an organic matrix. These mesoscopic structures form the basis for macroscopic morphologies whose hierarchy of structure depends on their spatial arrangement, shape, and relative volume fraction of HNP and free matrix.

core and the corona), and polymeric core–shell particles with cross-linked outer shells.

Within even this narrow definition, and focusing on self-suspended or "neat" HNPs, the parameter space is immense, and the opportunities to create useful structures and materials are enormous. The variables that can be "tuned" include: (i) the chemistry of the core (metal, semiconductor, magnetic, chalcogenide, amorphous or crosslinked carbon macromolecules, and proteins); (ii) the shape of the core (spheres, rods, disks, and other novel shapes), and the size of the core (the radius $R_0$, the aspect ratio $\alpha$ for disks and rods), which plays a role in both the mechanical properties of the hybrids as well as phenomena such as quantum confinement and photonic effects; (iii) the graft density of the corona $\sigma$; (iv) the nature of the graft (covalent or ionic); (v) the composition of the corona (polymer, oligomer, block copolymer (BCP), dendron, biomacromolecules, or liquid crystal mesogen); and (vi) the size of the corona (most commonly the molecular weight or degree of polymerization of the corona). By manipulating this parameter space, there exists a vast potential to realize a wide range of functional materials with controllable structure and properties.

We start by reviewing a series of theoretical and experimental studies with emphasis on the structure and dynamics of HNPs. With this guidance, we then discuss the synthetic approaches available and what key innovations are necessary to fully exploit their potential.

## Structure of HNPs and HNP assemblies

The major determinant of the interaction between HNPs is the conformation of the corona. At a coarse-grained level, the behavior of HNPs in solution is that of the soft-repulsion colloid model, where the particles interact through a distance-dependent repulsive potential that decreases with distance from the core.[17] Other examples of soft colloids are star polymers,[17,18] BCP micelles,[17,19] and superparamagnetic particles in a varying external field.[20] The closest analogy to HNPs are star polymers, and much of the behavior is expected to follow the same theoretical framework. The Daoud–Cotton model for star polymers predicts that for a star with number of branches $f$, each with a degree of polymerization $N$ and a Kuhn length of $l$, there exist three regions—a melt-like core whose radius is $r_{core} \sim f^{1/2} l$; a concentrated polymer brush (CPB) region where the polymer brush is stretched; and a semidilute polymer brush region (SDPB) with a radius that scales roughly as $R \sim N^{3/5} v^{1/5} f^{1/5} l$.[21,22] In the presence of a solvent, this swelling is due to the solvent, but in the melt state, the "solvent" consists of the arms of the surrounding stars.[17] This model has been explicitly modified by Ohno et al.[23] for an arbitrarily sized core and arbitrary grafting density, thus making it applicable to HNPs, and the same scaling behavior is seen, with an additional scaling due to graft density [Fig. 1(a)]. A significant feature of their extension is the critical radius $r_C = r_0 \sigma^{*1/2} v^{*-1}$ where $\sigma^*$ and $v^*$ are the reduced grafting density and reduced excluded volume parameter. This critical radius determines the transition of the corona from the CPB regime to the SDPB regime, and is an important parameter in determining the interaction of solid HNP assemblies, as will be seen later. A similar transition from CPB to SDPB, and the associated scaling behavior is found in the polymer graft model described by Milner, Witten, and Cates as modified for curved surfaces by Wijmans and Zhulina.[24,25] It is worth noting that these models also apply to BCP micelles in a selective solvent, thus making them analogous to HNP systems as well.[17] Here, the size of the less-soluble block, the chemical structures of the two blocks, and the selectivity of the solvent toward each block determines the core size and grafting density. The corona then consists of the more soluble block, which faces outwards.


https://doi.org/10.1557/mrc.2013.9 Published online by Cambridge University Press

Using the Daoud–Cotton star polymer model, Likos et al. developed an effective interaction potential for stars in the limit of large $N$,[18,26] thus exploring the length scale where each star can be treated as a separate spherically symmetric atom with an effective interaction potential. They then used this model to explore the phase diagram of star polymer solutions using Monte Carlo simulations[27] and found a number of crystal structures, including face-centered cubic (FCC), body-centered cubic (BCC), and diamond lattices. An explicit treatment of HNPs in good solvents by Kim and Matsen[28] using a self-consistent field theory bears out the general assumption that in the densely grafted limit, the interaction potential for the particles is purely repulsive, and is soft when the two particles begin to impinge on each other. These methods of inherent structure formation resulting from corona-mediated potentials open up new avenues (complementing mesophase-templated concepts such as BCP-nanoparticle blends) yet to be fully explored to create ordered, organic–inorganic superlattices.

In densely packed, highly grafted systems, the structures obtained are very much what one would expect for colloidal spheres. For example, Goel et al. investigated systems consisting of silica nanoparticles grafted with poly(*n*-butyl acrylate) brushes with graft densities of around 0.8 chains/nm$^2$ [Fig. 2(a)]. SAXS measurements determined that the structure factor $S(q)$ showed two peaks with $q_1{:}q_2{::}1{:}3^{1/3}$, and a weak peak at $7^{1/2}q_1$, indicating an FCC or random close-packing structure. Transmission electron micrographs of thin films show the hexagonal arrangement expected from such a polycrystalline structure. The distance between the particles scales as $N^{1/2}$, as expected for a star polymer-like system [Fig. 2(b)].[29] The bulk materials are solids with elastic relaxation times greater than $10^5$ s, while the hair, when unattached to particles, show liquid behavior with relaxation times less than 1 s. The bulk material shows a distinct yield stress, much like colloidal crystals or ordered BCP structures.[30] As the interaction potential between adjacent HNPs would not only affect the structure but also the elastic properties, they examined the scaling of the elastic modulus with the molecular weight of the polymer (and hence the radius) and determined that the repulsive potential scales as $U(r) \propto r^{-12.5\pm2}$, unlike the star polymer exponential potential derived by Likos et al.[18,26] a difference they attribute to the effect of the finite core.[29]

The soft-colloid/star polymer model assumes that the following conditions are valid—that particle interactions are pairwise additive, and that there is either a solvent or free homopolymer (that acts as a Θ solvent) that swells the brush. Yu and Koch[31] argue that in the solvent-free limit, the interaction potentials are no longer pairwise additive, due to the constraint that polymer molecules tethered to particles would seek to fill all interstitial voids between the spheres surrounding the particles. If the length of the brush is of the order of the radius of the particle, this creates a multibody problem. Using a density functional theory, they simulate the structure factor $S(q)$ and find that $S(q=0)=0$. From this they postulate that HNPs behave as incompressible single-component fluids rather than a suspension of spheres. Chremos et al. compare a modification of this model (with the incompressible fluid replaced by a Lennard-Jones fluid) with molecular dynamics (MD) simulations. These simulations explicitly model the HNPs as spheres covered by polymer chains of Lennard-Jones spheres joined by harmonic springs.[32] They find that at low temperatures the earlier model of an incompressible fluid holds. At higher temperatures, the dynamics of the end groups of the polymer chains are found to act as an unconnected solvent, swelling the brushes and therefore validating the soft-sphere models under these conditions. However, attempts at coarse-graining the MD models to develop effective interaction potentials at lower temperatures and shorter chain lengths have met with limited success.[33]

Chremos and Panagiotopoulos[34] then use this MD model to investigate the structural transitions of these materials as a function of grafting density, core size, and temperature, and demonstrate that the HNPs can form glasses, isotropic aggregates, anisotropic aggregates, and star fluids [Figs. 2(c) and 2(d)]. The isotropic aggregation they see is the solvent-free equivalent of the structures seen by Akcora et al.[14] in experiments with polymer-grafted nanoparticles dispersed in homopolymer matrices. While the aggregation is thermoreversible in simulations, the surface chemistry of the nanoparticles (not taken into account in the simulations) may prevent redispersion of the particles, thus offering a way to engineer structure formation within HNP assemblies by varying graft density and core size.

The soft colloid models emphasize repulsive interactions. Some attractive force is required, however, to build large, stable assemblies of HNPs. In the absence of external stimuli such as magnetic and electrostatic fields, assemblies of HNPs can be held together in three ways; dispersion (van der Waals) interactions at the outer surface of the corona, chemical interactions between functional groups at the outer surface of the corona, and physical entanglement of the corona.[35] When the corona is of a length that does not allow it to transition from the fully stretched CPB regime (i.e. it remains "dry" with respect to the corona of neighboring particles), the resulting material is an assembly of hard spheres, and consequently brittle due to the relatively weak dispersion interactions between the HNP corona peripheries. Corona entanglement, on the other hand, creates a more robust assembly alternative. Experiments on poly(methyl methacrylate) grafted silica particles in a free-chain matrix have verified that mechanical reinforcement can occur due to corona-mediated bridging of the particles.[36–38] When the corona is in the SPDB regime, entangled brushes on neighboring particles enhance the toughness and fracture resistance of macroscopic assemblies of nanoparticles by dissipating the fracture energy via craze formation and plastic deformation, thus opening up the possibility of creating robust large arrays of nanoparticles.[39] Choi et al. determined that the brush dimensions follow the scaling laws described by Daoud and Cotton, and developed an expression for determining the



https://doi.org/10.1557/mrc.2013.9 Published online by Cambridge University Press

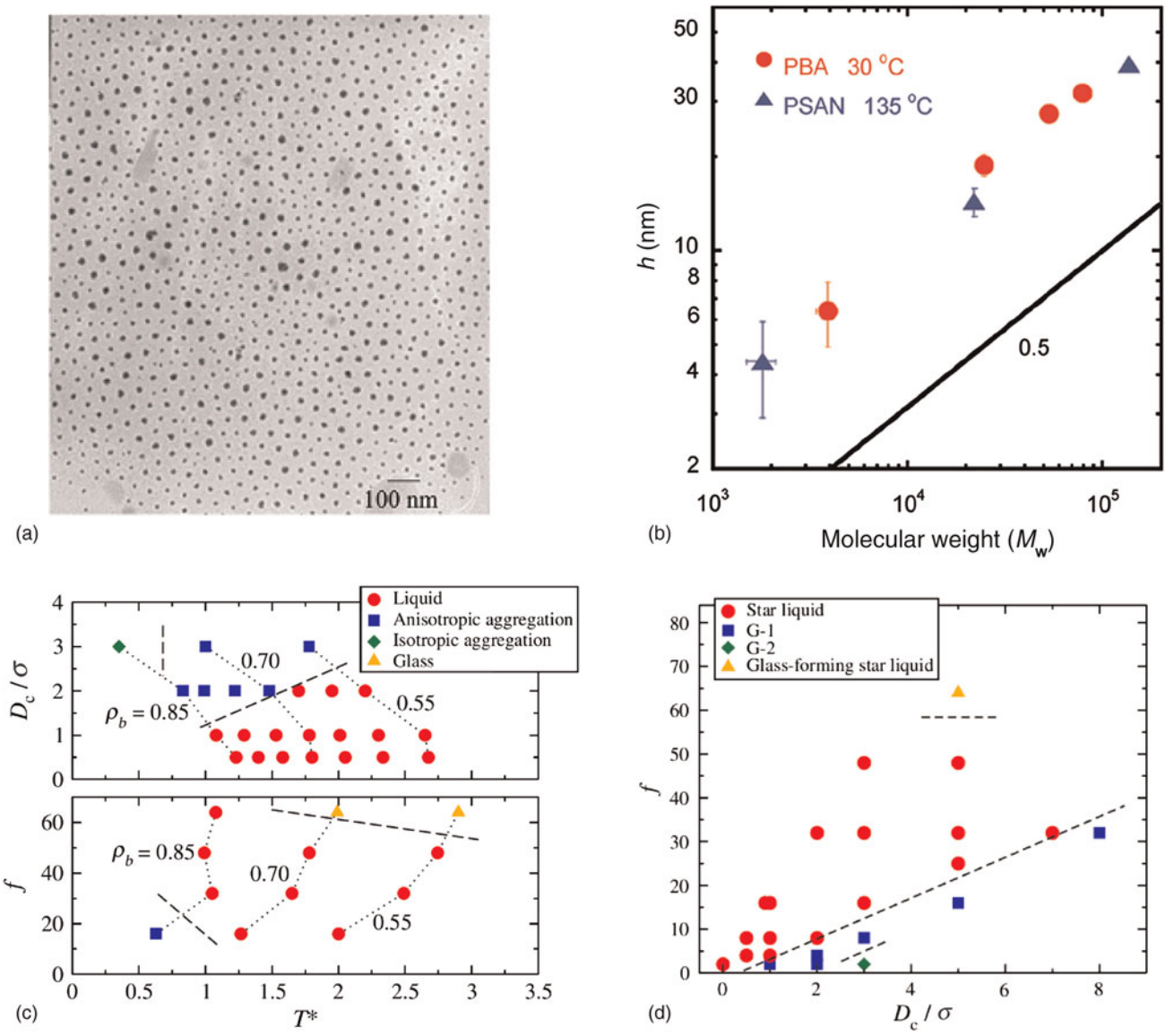



**Figure 2.** (a) TEM by Goel et al. of a solvent-free film of silica nanoparticles grafted with a poly (butyl acrylate) brush and (b) calculated brush height as a function of molecular weight for poly (butyl acrylate) and poly (styrene-co-acrylonitrile) brushes from the same study. ((a), (b) Reproduced with permission from Ref. 29, copyright 2011 American Chemical Society.) (c) Simulated phase diagrams of HNP assemblies showing a library of structures available as a function of (above) $D_o/\sigma$ (particle diameter/brush blob size) with four chains per particle and (below) number of arms per particle with $D_o/\sigma = 5$. The horizontal axis is reduced temperature. (d) Structural map of HNP assemblies from the same study as a function of arm number and $D_o/\sigma$ for a chain length of 10 monomers. ((c), (d) Reproduced with permission from Ref. 34, copyright 2011 American Physical Society).

minimum degree of polymerization of the hair needed to create toughened arrays. For films of particles with brush length $N$ greater than $N_{min}$ (about 600 for PS and PMMA brushes on 8 nm radius particles), the hardness and modulus are essentially the same as the linear polymer, and almost double the value for particles with shorter brushes. The fracture toughness increases by about 300% as the system transitions into the highly entangled regime, and is almost an order of magnitude higher than the linear polymer, due to the particles forming network points in the polymer structure, analogous to the physical crosslink points that enhance toughness in thermoplastic elastomers. They find that $N_{Min} = 2N_e + (a^{-1}[r_C - r_0])^{1/x}$, where $r_c$ is the radius at which the brush transitions from the CPB to the SDPB regime, $x$ is the scaling parameter for the concentrated region, $N_e$ is the entanglement length of the polymer, and $a$ is the segment length of the polymer. This expression offers a design guide to create toughened arrays of nanoparticles, since $r_0$ and $r_C$ can be tuned ($r_C$ is dependent on the graft density), and all the other variables depend on the choice of the polymer.[39]


https://doi.org/10.1557/mrc.2013.9 Published online by Cambridge University Press

At this point, it is interesting to note another possible toughening mechanism afforded by the synergism of corona entanglement *and* structural order—that of dislocation motion and boundary slip within the lattice, and between domains, of ordered HNP assemblies, respectively. Many conceptual analogies can be drawn between morphology and composition based strengthening concepts developed for metals and intermetallics and ordered assemblies of HNPs and mixtures thereof. For design and conditions that minimize entanglement and maximize the dynamics of the corona, the HNP, rather than the chain, will dominate the strain response and assemblies will deform by relative motion of HNPs via point, line, and plane defects within an ordered lattice. Unfortunately, assessment of the impact of these mesoscopic deformation modes is not currently possible as detailed studies of the conditions and transition between corona chain and HNP lattice deformation are unavailable.

Another possible method to toughen assemblies of HNPs is to have the hairs chemically interact, either reversibly or irreversibly. Agarwal, Chopra, and Archer report a shape memory material synthesized from HNPs by linking the hairs on adjacent particles with a covalent bond. In this case, they use a low molecular weight PEG (MW = 5 kDa) corona on silica particles. The outermost hydroxyl functional groups of the PEG brushes are then crosslinked using hexamethylene diisocyanate to form polymer bridges between nanoparticle "netpoints". The resulting materials "remember" the original shape of the film even after they are deformed on heating, due to the setting of the structure during synthesis.[40] Iyer et al.[41] have developed a model that tries to capture the mechanical behavior of such crosslinked systems with both irreversible (covalent) and reversible (ionic/hydrogen) bonds based on a variety of parameters, such as the proportion of reversible to irreversible bonds between particles. By tuning the proportion of reversible bonds to permanent bonds, and varying the interaction strength of the reversible bonds, it is possible to change the yield behavior from ductile to elastic. This change could be achieved, for example, by using end-functionalized polymers with varying ratios of polar and reactive groups.

While most HNP systems are designed to minimize contact between particles, for some purposes the controlled aggregation seen above can be essential to create multifunctional nanocomposites. Torquato, Hyun, and Donev have looked at the optimization of multiple properties in multiphase systems, where each component has a different optimal property. By using electrical and thermal conduction as the two properties to be simultaneously optimized, they have shown that the ideal structures are interconnected networks.[42] Guest and Prevost[43] have found similar results for the simultaneous optimization of stiffness and permeability. Formation of these interconnected networks can be achieved with BCPs, but in the event that one of the functionalities requires an inorganic component, it is necessary to have a library of structures where the nanoparticles are selectively aggregated. BCP-templated nanocomposite structures, in which nanoparticles are forced into specific domains, have been reported both in simulations[44] and experiment,[45–47] but they have the same limitations as the conventional nanocomposites mentioned in the introduction (mixing, agglomeration and low inorganic volume fractions). An alternative route is to use HNPs where the hairs are BCPs[48,49] or liquid crystal mesogens[50,51]. This design allows for much more controlled structure formation (Fig. 3): BCP-tethered HNPs have been used by multiple researchers to create complex structures such as tubules and vesicles with walls built out of HNPs,[52] as well as lamellae and "segmented worms."[53]

Jayaraman and Schweizer used a modified version of the polymer reference interaction site model to investigate structure formation for particles with very low graft densities; 1, 2, 4, and 6 polymers per particle.[54–56] Systems with 1 and 2 chains per particle are analogous to di-block and tri-block copolymers, with the nanoparticle forming one of the blocks, and results of these simulations, as well as computational studies by Iacovella, Glotzer, and others show the same micellar, lamellar, and interpenetrating gyroid structures seen in copolymer systems (Fig. 3).[56–58] Similar surfactant/BCP-like behavior has been seen experimentally with Janus particles, where opposite sides of the particles are coated with different ligands.[59] The vast majority of the BCP-tethered and low-graft density tethered HNP structures, however, are only now being verified experimentally, making this a rich field for experimental work.

While most of the work described here is for spherical nanoparticles, a wide variety of particle shapes have been reported, including rods, bars with various cross-sections, cubes, and other faceted 3D structures, circular disks, and plates with varying numbers of sides.[60] More complex shapes, such as stars[61] and dumbbells,[62] have also been reported. While it can be argued that some of the behavior of the corona would be similar, very little work, computational or experimental, has been done on HNPs with structures other than spheres, rods, and disks. Glotzer et al. have performed computational studies on anisotropic particles with a low graft density[63,64] as well as on ungrafted anisotropic particles,[65] and they report the formation of various lamellar and packed column phases, but there has been to date little experimental verification of these results, making this another potentially fertile avenue for experimental work.

An alternative approach to structure formation is to use HNPs with selectively active coronas. By creating binding sites that have lock-and-key reactivities, it is possible to exert finer control over the precise spacing of particles. For example, Nykypanchuk et al. exploit base-pair complementarity of DNA ligands to create BCC crystallized gold nanoparticles with defined ordering of particles.[66] This form of complementary functionalization has also been reported with peptide ligands.[67] Glotzer et al. have simulated the assembly of "patchy" isotropic and anisotropic particles that could be experimentally realized with functional ligands, and have found an extremely rich gallery of superlattices that point the way to metamaterials of the future.[68] However, detailed theory that reveals the balance between intermolecular



https://doi.org/10.1557/mrc.2013.9 Published online by Cambridge University Press

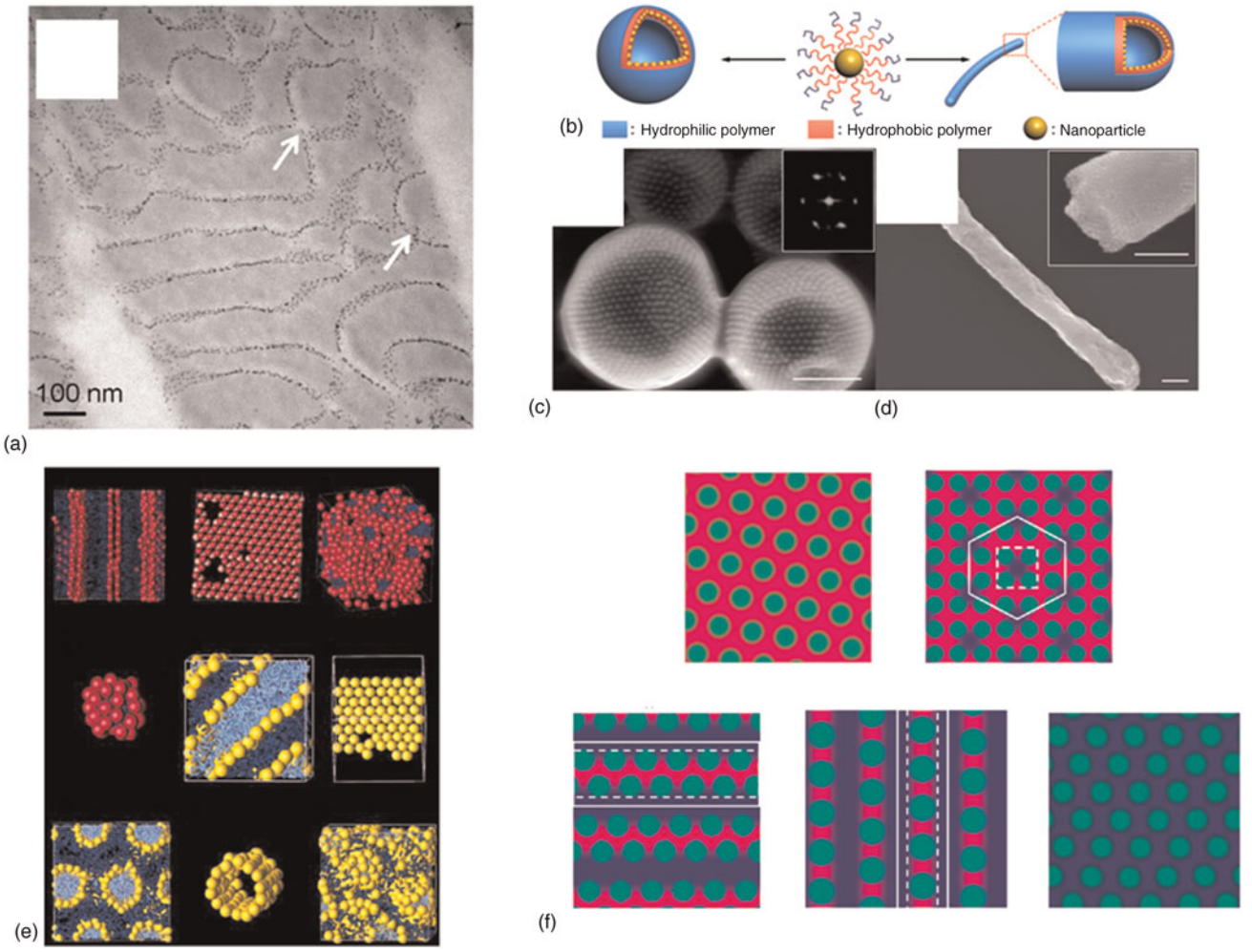



**Figure 3.** Examples of controlled aggregation of HNPs using BCPs, liquid crystals, and single polymer grafts. The aggregates are solvent free or slightly swollen HPN assembles. The hierarchical morphology arises from interactions between these structures, the volume fraction of constituents and details of process techniques and history. (a) TEM of lamella formed by triblock copolymer tethered HNPs. (Reproduced with permission from Ref. 53, copyright 2011 American Chemical Society.) (b–d) Vesicles and tubules formed by BCP-tethered HNPs. (Reproduced with permission from Ref. 52, copyright 2012 American Chemical Society.) (e) Simulations of phases formed from singly tethered nanospheres. Top row, left to right: Lamellar phase; End on view of lamellar phase; micellar phase. Middle row: Single micelle from previous; lamellar phase; single lamella from previous. Bottom row: Cylindrical phase; single cylinder from previous; another spherical micelle phase. (Reproduced from Ref. 64, copyright 2003 American Chemical Society.) (f) Simulations of BCP-tethered nanoparticles. The A block is blue, the B block is red, and the particles are green. In order of increasing A block proportion, the phases are cylindrical (top row), lamellar (bottom row, left, and center) and cylindrical (bottom right). (Reproduced with permission from Ref. 48, copyright 2010 American Chemical Society).

specificity (such as afforded by bimolecular recognition motifs) and an effective soft potential between two coronas on the symmetry of the final structure is still in its infancy. For example, the same chains, sheets, and BCC packing have been observed in experiment[14] and in simulations using effective interaction potentials[27,69] rather than relying on complex biomolecular complementarity.

## Dynamics of HNPs and HNP assemblies

When HNPs are considered as colloids with spherically symmetric softened potentials, the dynamics of solvent-free assemblies above the glass transition temperature ($T_g$) of the corona can be expected to follow a similar framework. For example, the same kinetically trapped soft glasses seen in star polymers[26,70,71] can also be seen in concentrated HNP systems.[72] The relaxation modes and spectrum of a polymer chain depend on both intra-chain connectivity and the local packing of near neighbor chain segments. For HNPs, the latter will depend on the molecular weight and graft density of tethered chains, as well as on the distance from the core surface (due to core curvature). Thus, for the same ratio of core-to-corona volume, drastically different dynamics of individual chains, the corona, and HNP assembly may be expected. Therefore, for similar HNP compositions a range of thermomechanical responses, including $T_g$, viscosity, melt extensibility, tenacity, and physical aging are expected.


https://doi.org/10.1557/mrc.2013.9 Published online by Cambridge University Press

Following the discussion above on chain structure in the corona, the dynamics of individual chains will depend on the curvature of the surface in which they are tethered. Savin et al. measured the molecular weight dependence of $T_g$ of the corona of HNPs with high graft density compared with the glass transition temperature of the free polymer,[73] and found that the $T_g$ of the corona is higher than that of the free polymer, but approaches it as the molecular weight increases. Since $T_g$ of a polymer is related to the freedom of the polymer to relax, shorter chains and higher graft densities result in stretched and constrained chains (with a greater proportion of the polymer in the CPB regime) which are unable to relax, raising $T_g$. With increasing molecular weight, the proportion of the chain that is in the semidilute (SDPB) regime increases, and the $T_g$ approaches that of the free polymer. For lower graft densities, particle–polymer interactions responsible for packing frustrations of freely jointed chains at a curved surface could lead to either an increase or decrease. For example, Tchoul et al.[74] showed that the $T_g$ of 100 kDa PS tethered (0.03 chains/nm$^2$) to $TiO_2$ ($r = 18$ nm, $l = 40$ nm) decreased by 30 °C relative to the bulk, even though $TiO_2$ is close to a neutral surface to PS. Thermal cleavage of the tethering point restored the $T_g$ to that of the bulk, implying the suppression was due to excess free volume arising from frustrated chain packing. Packing frustration due to interstitial spaces within HNP assemblies that were pointed out by Yu and Koch[29] should have a profound impact on other collective relaxation modes, such as physical aging. Such detailed studies on HNP assemblies, crucial for long-term use assessments and processing procedures to tune order (i.e. solvent and/or thermal annealing) are not currently available; however, studies on other soft colloid assemblies, including multi-arm stars, provide a starting point.

One of the more novel areas in which HNPs have been used is in creating solvent-free fluids of nanoparticles.[75–77] Under conditions when the hairs in the ungrafted state would be a liquid, the corresponding HNP systems, in a solvent-free state, range from simple liquids to waxes depending on the hair length and the graft density.[75] With small cores and large polymers ($R \ll R_g$), HNPs behave as star polymer melts (as expected), and follow the dynamics of star polymers.[78] When the hairs are so long that their ends are in the semi-dilute regime, the outer portion of the corona is only weakly correlated with the cores, and the particles can be considered to be self-suspended (as described earlier by Yu and Koch).[31] When the hairs are extended in the brush regime, but are not so long that the ends are in the semi-dilute regime, the corona is closely correlated with the core, and the HNP system would behave as a soft glass. This model has been confirmed by molecular dynamics simulations[79] and by rheological measurements.[75]

Increased fluidity is found in a particular class of HNPs—known as Nanoparticle Ionic Materials (NIMs) where the bonding of the corona to the core is ionic in nature.[76,77,80–82] MD simulations suggest that even though the ionic bonds between the corona and the particle are stronger than thermal energy, the hairs are able to hop from particle to particle, offering an additional relaxation mode.[83] This hopping effect dominates the intermediate scale dynamics (10 s of nanoseconds), while NMR studies show that the fast dynamics (nanoseconds) of the hairs are essentially unchanged.[84] At the same time, particle diffusion (in the 100 s of nanoseconds timescale) is found to be faster for a covalently tethered corona as opposed to the ionically tethered one. This finding suggests that the increased fluidity of NIMs is due to the ability of the hairs to move from particle to particle and offers a useful method to create materials that flow as liquids while retaining a high inorganic content.

## Synthetic strategies for HNPs

In general, the synthesis of HNPs involves three steps: (i) Synthesis of nanoparticle, (ii) synthesis of the corona, and (iii) attachment of the corona to the particle. There are a few basic strategies in combining these steps (Fig. 4): (i) Synthesize the nanoparticles in the presence of the corona; (ii) synthesize the nanoparticles and corona separately, and then attach the corona to the particles (grafting-to); and (iii) synthesize the nanoparticles, and then grow the corona from the surface of the nanoparticle (grafting-from). Each of these strategies presents its own challenges, but the most critical challenge (for all three) is achieving monodispersity and purity with high yield (and volume). The synthesis of monodisperse particles and polymers are challenging fields in their own right, and combining them brings a fresh set of challenges to the table. For fundamental studies and some applications monodispersity of all constituents and design parameters is critical, hence, overcoming these challenges is a priority.

Several strategies exist for synthesizing large quantities of monodisperse nanoparticles.[85,86] Choosing a synthetic route requires considering the properties of the particle surface as well as the conditions needed to add the corona. The particle must be readily dispersible in the solvent that the corona addition or growth takes place in. In addition, if the solvents for nanoparticle synthesis and polymer synthesis are incompatible (for example, aqueous solution for nanoparticle synthesis and toluene for polymer growth) it may become necessary to incorporate a stabilizer that allows the nanoparticles to be removed from one solvent and dispersed in the other. These stabilizers must then be incorporated into the corona or removed by ligand exchange. This method is used, for example, in the Brust synthesis of gold nanoparticles, in which the precursors are mixed in an aqueous phase and then extracted into an organic solvent by using a surfactant.[85] In some cases the stabilizer selected can be the desired corona—for example, BCP micelles can be loaded with metal ions that are then reduced to form metallic or silica nanoparticles that are coated with the polymer.[87,88] The organic, however, limits the postprocessing temperature for the inorganic; so in many cases the highly crystalline, low defect semiconductors or oxides that are necessary for high-quality optical and electronic devices are not achievable.



https://doi.org/10.1557/mrc.2013.9 Published online by Cambridge University Press

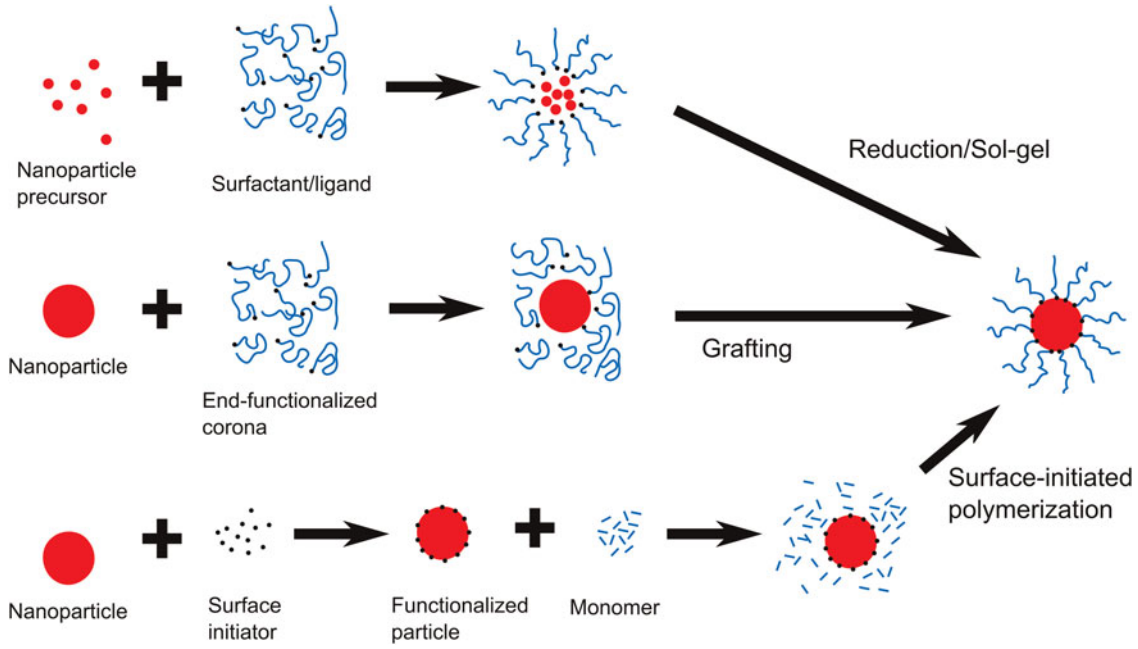



**Figure 4.** General synthetic routes to HNPs (top to bottom): synthesize the nanoparticles in the presence of the corona; synthesize the nanoparticles and corona separately, and then attach the corona to the particles (grafting-to); and synthesize the nanoparticles, and then grow the corona from the surface of the nanoparticle (grafting-from).

While most of these methods are used to synthesize spherical particles, there are techniques to synthesize cubic, bar, rod, disk, and plate-shaped particles.[60] More complex shapes (such as stars) have also been synthesized and characterized. With the rich variety of structures and applications possible for spherical particles alone, it is obvious that the addition of particle shapes will increase the available design space. Regardless of the diversity of approaches and concepts available to create nanoparticle cores, the requirement to add a molecularly designed corona in a scalable manner with control over chemical and structural dispersion places substantial constraints on the synthesis technique chosen. It is essential to maintain conditions compatible with controlled chemical synthesis and particle dispersion in order to obtain a well-behaved HNP system as a final product. Any aggregation before corona attachment will often translate to aggregation after attachment, leading to uncontrollable side-products with poorly defined properties.

In all HNP routes, consideration of the organic–inorganic coupling is crucial. There are a number of attachment strategies, depending on the surface of the nanoparticle. Metal and metal oxide particles, in particular, have been widely studied and there are multiple chemical modifications that have been shown to work.[89–91]

For gold and noble metals, possibilities include thiols,[67,92–94] tyrosine and disulfides (which cleave to create a thiolate link), amines, carboxylates,[95] pyridine, and phosphines. These links are relatively weak (and can provide a path for ligand exchange; phosphines and amines can be exchanged for thiols) but can be strengthened by using multiple linkages, either of the same (such as polyphosphines) or different types. An amino-acid terminated ligand, for example, may have one or more of amine, thiol, and carboxylate groups available for bonding to the surface, with a corresponding increased ligand binding due to the multidentate nature of the interaction.

While the same groups can be used for the modification of metal oxide nanoparticles, more typical routes involve using a silane, carbonate,[89] or phosphonate-terminated ligands. Silanes condense with the –OH groups on the surface to form a strong Si–O bond. This synthesis has been shown to be effective for a variety of oxides, including $SiO_2$, $HfO_2$, and $TiO_2$, and is the method of choice for functionalizing silica particles, as the Si–O–Si bond formed is particularly stable. However, the silane may self-condense, thus making grafting difficult to control and the grafted layer ill-defined. In contrast, phosphonate-terminated ligands (with the terminal group being P–OH, PO–alkane, or $P–O^-$) resist self-condensation, forming a single layer on the surface, and form particularly strong bonds with titania (though not with silica). Both silanes and phosphonates can form multidentate bonds, with up to three M–O–Si or M–O–P bonds per ligand (where M is the nanoparticle element).

As noted above when using separately synthesized nanoparticles, there are two broad strategies available for adding a corona. "Grafting to" involves the attachment of a pre-synthesized corona. Separating the corona synthesis step allows for greater control over corona synthesis and purification without having to simultaneously maintain the nanoparticles in solution. However, there are a number of potential issues with the grafting-to strategy. The first is that the grafting density is


https://doi.org/10.1557/mrc.2013.9 Published online by Cambridge University Press

inherently difficult to control; the reactive terminal group of each additional corona molecule has to diffuse past the already assembled corona to attach to the surface. This limitation slows the grafting kinetics to logarithmic time once the graft density is high enough for the corona near the particle surface to enter the concentrated brush regime.[96] In addition, the number of chains per particle is not constant in a typical synthesis procedure—Oyerokun and Vaia[97] showed that the chain distribution is Gaussian and becomes wider as the polymer increases in size relative to the particle. Another limitation is the synthesis of the polymer with the appropriate terminal group—for example, alkoxysilanes and chlorosilanes are reactive, and may not be compatible with the polymerization techniques preferred or the backbone of the polymer. A detailed examination of polymer synthesis strategies is outside the scope of this perspective, so we will simply note that the objective is to synthesize the polymer with a more easily accessible terminal group, and then to either modify the end group, or to first modify the particle surface, and then bond the polymer to the modified particle. A good example of this approach was demonstrated by Hübner et al.[98] who grafted anionically grown 1,4 polybutiadiene to chlorosilane functionalized silica nanoparticles. Their study also highlights the drop in graft density as molecular weight increases. This two-step approach also tackles the issue of uniformity, since the first graft step involves moieties that are small compared to the nanoparticle, leading to a narrower graft number distribution.[97]

An interesting variation on the two-step "grafting to" approach is the synthesis of NIMs, where the interaction between the polymer and the surface-modified particle is ionic rather than covalent, creating a molten nanoparticle/polymer salt.[76,77] The ionic approach has one remarkable advantage—the strongly ionic groups on the nanoparticles keep them stable in polar solvents until polymer addition is complete. This method has also been used to tune the interaction strength between the brush and the nanoparticle beyond the tridentate bonds possible with silanes and phosphonates; sulfonate-stabilized $CaCO_3$ particles were reacted with an ABA BCP, where the B block was a polyamine with a controlled number of amine groups.[97,99] This approach can also be used when the charged groups are inherent to the particle, such as for polyhydroxylated fullerenes[100] and colloidal silica.[101]

The alternative approach, "grafting from", allows separate tuning of the grafting density and graft molecular weight, due to the increased diffusivity of monomers relative to the full-length chains. This approach involves first attaching an initiator molecule to the surface of the particle using the attachment techniques listed above, and then growing a polymer from the initiator. Since the initiator is a small molecule, high graft densities (up to 4–5/nm$^2$) and more uniform distributions can be achieved, and then a proportion of the initiators can be blocked to achieve a controlled graft density. This approach allows for higher graft densities with larger molecular weights than the "grafting to" method, since the growing end of the polymer is exposed to (or very close to) the monomer-containing solvent.[102] A chain-growth polymerization technique is necessary in order to prevent cross-linking of adjacent brushes. Ideal polymerization techniques should have low self-termination rates, in order to achieve a high and controllable degree of polymerization and low polydispersity. These criteria are satisfied by a range of techniques,[103] including controlled radical polymerizations,[104] and living anionic[105] and cationic[106] polymerizations. Living ionic polymerizations, however, require extremely pure reagents and solvents, and so can be problematic when dealing with nanoparticles that may have trace impurities. These restrictions also prevent living ionic polymerization from being a viable technique for cost-effective mass production of HNPs. Finally, another criteria for choosing a technique would be the compatibility of the polymerization reaction conditions with conditions that keep the nanoparticles unaggregated while the corona is building.

Two of the most widely used grafting-from techniques are Atom Transfer Radical Polymerization (ATRP)[104,107–109] and Reversible Addition Fragmentation Transfer (RAFT)[110]. These are both mechanisms that are tolerant of a wide variety of functional groups on the monomer, greatly expanding the library of coronas available for HNP synthesis. Surface-initiated ATRP involves the grafting of an initiator (terminated with a halide) to the nanoparticle, and then carrying out the polymerization in the presence of an ATRP agent, a transition metal catalyst that later needs to be removed. While conventional ATRP is sensitive to the presence of oxygen (due to the oxidation of the ATRP agent), Matyjaszewski et al.[108] have developed a variant known as ARGET-ATRP that is much more tolerant to harsh conditions. ARGET-ATRP can be started with residual air in the reaction vessel—reducing agents regenerate the transition-metal activators that are initially oxidized by residual oxygen—and the reaction stops when exposed to air again. This ease of control, and the small amounts of transition metal complexes needed for growth make surface-initiated ARGET-ATRP a particularly attractive method for synthesizing large quantities of HNPs. RAFT is another highly versatile technique that requires mild conditions and offers a wide range of monomers and solvents to choose from.[110] Benicevicz et al. were one of the first to establish a grafting-from route for HNPs using RAFT-silane agents to functionalize silica and polymerize PS and PMMA at high yields while controlling graft density and molecular weight of grafted chains.[111,112] RAFT offers one major advantage over ATRP: it uses a thioester RAFT agent as opposed to a transition metal ATRP catalyst, eliminating the heavy metal contamination of the final product. However, due to kinetic considerations, it is necessary to have a large excess of RAFT agent (in addition to the one tethered to the particle) in the reaction mixture, which leads to a significant amount of free polymer forming in the solution that must later be removed by a purification step. ATRP[107] and RAFT[88] have also been used to synthesize HNPs in a one-pot synthesis by a variety of approaches. This approach is particularly suited for all-organic



https://doi.org/10.1557/mrc.2013.9 Published online by Cambridge University Press

HNPs; first creating BCP micelles[110] or stars,[113] and then crosslinking the inner block to form the rigid particle.

In summary, there have been a number of techniques developed for synthesis of monodisperse size-controlled nanoparticles, with a controlled graft density and corona size and architecture. The library of particles that are available is enormous, and it is essentially possible to create any combination of particle and corona provided one chooses the right chemistry and conditions. The choice of architecture, therefore, is determined by the intended application. Surprisingly, a single comprehensive correlation between synthetic approaches, their limits and a framework based on physics (as summarized above) is lacking. For example, what HNPs (composition, molecular weight, and graft density of the corona) can be created with many, or only a few approaches? What are their relative advantages? Current development efforts are based more on synthetic approaches at hand, rather than on a self-consistent analysis of limitations of various methods and the necessary HNP structures determined by the underlying physics. Nevertheless, many applications demand a combination of purity, monodisperity, volume, and cost that cannot be achieved with current technologies outside of the specialist's research lab. The lack of throughput, yield, purity, and robust HNP design tools that enable optimization of property-processing-synthesis trade-offs are pervasive, and one of the major challenges currently limiting wide applications of neat HNPs to high value technologies.

## Future prospects in applications of neat HNP systems

The wide parameter space available for architectural choices for neat HNP systems opens up an equally large application space. Some uses of HNPs can be seen as "nanocomposites-plus" where HNP assemblies are drop-in substitutes for the same applications as earlier dispersed-particle nanocomposites, with the potential for greater structure control and phase stability. However, the possibility of modular design of the organic and inorganic components to provide high inorganic loadings with polymeric processibility allows for additional applications that would not have been otherwise possible. It is reasonable to expect that emerging HNPs will significantly impact future opportunities from energy and power management to multifunctional bulk structures, coatings, lubricants, optical films and sensors.[114]

Arguably the most important characteristic of neat HNPs with respect to technology integration is the ability to process hybrid materials without the issues of agglomeration and aggregation. This opportunity greatly expands manufacturing options. The potential design flexibility of HNPs affords several opportunities for many different traditional (e.g., extrusion, protrusion, melt compounding, thermoset cure, film blowing, solution coating, lithography, etc.) and emerging (additive manufacturing, nano-imprinting, etc.) processing methods. For example, using an entanglable thermoplastic corona, the resulting HNP assembly (exhibiting magnetic, dielectric, optical, or any other functionality) can be heated and formed into a desired shape [Figs. 5(a) and 5(b)]. HNPs with thermoplastic coronas are suitable for integrating with emerging additive manufacturing techniques, such as fused-deposition 3D printers. More dynamic corona designs using varying molecular architectures and chain lengths [Figs. 5(c) and 5(d)] can lead to HNP fluids that can be used as inks in roll-to-roll processing to print various functional patterns. In addition, reactive coronas can allow radiation induced cross-linking and pattern formation via lithography.[115] In this way, it is possible to create extended structures with inorganic functionality without reaching the high temperatures required for inorganic 3D printing.

To complement bulk and coating processibility, HNP design modularity is also very attractive for synthesizing films with complex structures using techniques, such as layer-by-layer assembly. By using ionic groups on the periphery of the corona, it is possible to deposit in a self-limiting manner alternating layers with alternating charges on a charged surface. So far, this approach has been used principally with a single type of nanoparticle alternated with layers of polyelectrolytes with the opposite charge,[116,117] to create polymer–nanoparticle films for a variety of applications including multicolored quantum dot films,[118] switchable conducting membranes,[119] biocidal and antifouling coatings,[120,121] superhydrophilic coatings,[122,123] and photovoltaics,[124] among others. However, the use of functional HNPs could provide finer control and greater functionality, with each layer consisting of a neat HNP assembly. For example, photovoltaic applications need layers of donor and acceptors in close contact, a feature that would be easy to achieve with a layer-by-layer assembly.[125] This approach can also be used to create nanoparticle "fabrics" only one particle thick and centimeters long that are ordered and crosslinked assemblies of HNPs.[126,127]

The choice of corona functionality offers incredible versatility to tailor neat HNP properties in addition to their processability. Rather than simply providing a matrix for the nanoparticles, the corona can bear chemical functionality with some level of reactivity toward external gases or liquids, thus integrating chemical responsivity to the hybrid. One such application is the growing field of carbon dioxide capture. Conventionally, $CO_2$ capture is carried out by low molecular weight amines that evaporate easily and are corrosive. As seen above, with the correct choice of polymer, it is possible to create self-suspended nanoparticle fluids that resist aggregation and phase separation. By tethering the organic component of the capture fluid (such as a polyethyleneimine) to nanoparticles, it is possible to create a material with tunable viscosity that has improved thermal stability.[128] The absence of any untethered solvent gives these fluids zero vapor pressure, allowing them to be used without issues arising from evaporation. In addition, entropic effects in the structural ordering of the corona were found to improve uptake capacity relative to ungrafted polymers.[129] This concept can be extended to other flue gases, such as $SO_2$, $NO_2$, and CO. It is worth noting in passing that the concept of using HNPs for environmental remediation


https://doi.org/10.1557/mrc.2013.9 Published online by Cambridge University Press

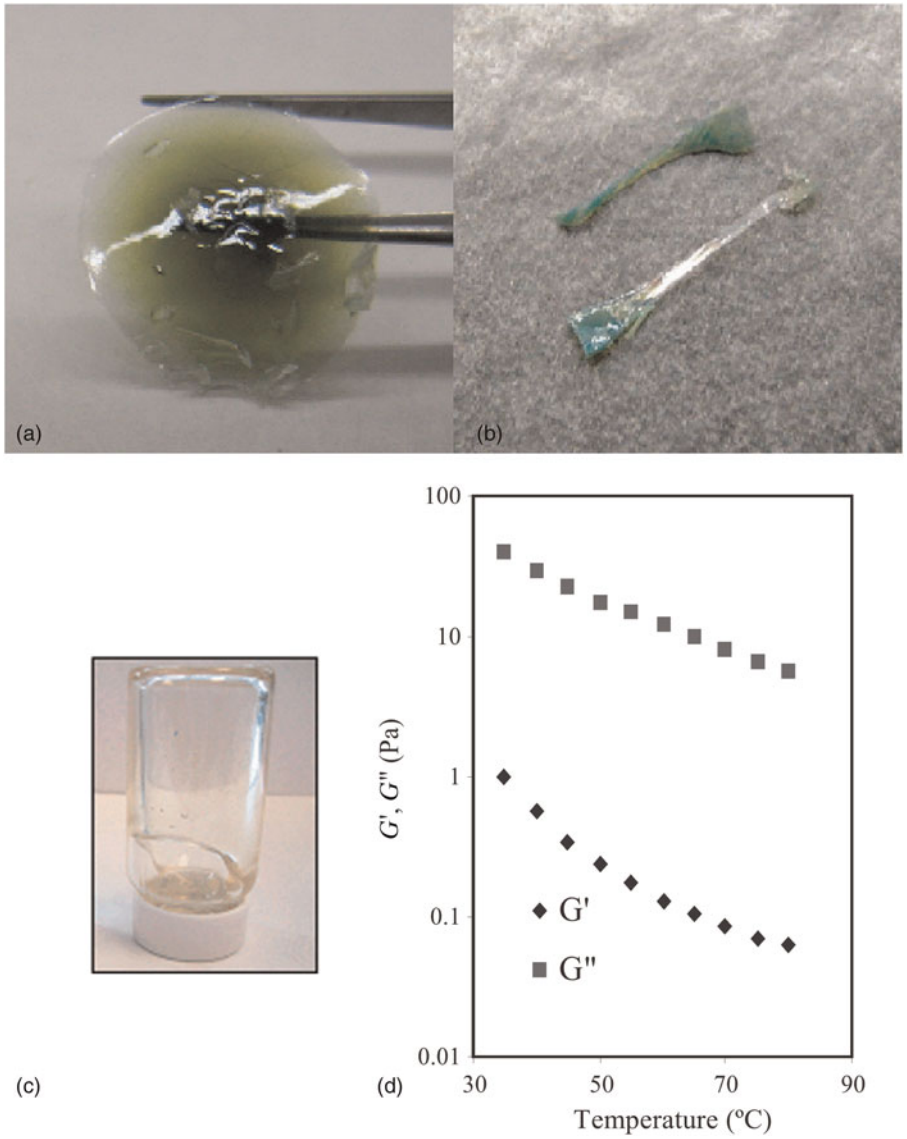



**Figure 5.** Deformability of bulk HNPs. (a, b) Titania/polystyrene (100 kDa) HNPs from Ref. 74, immediately after solvent evaporation (left) and after heating above $T_g$ and stretching (right). (Reproduced with permission, copyright 2010 American Chemical Society.) (c) Image of solvent-free silica NIMs and (d) temperature dependence of oscillatory shear moduli showing liquid behavior ($G'' > G'$) from Ref. 74. (Reproduced with permission, copyright 2005 John Wiley & Sons).

is not limited to solvent-free assemblies. For example, magnetic nanoparticles with oleophilic coronas can be deployed into an oil spill, where the corona would absorb the oil, and are then collected with a magnet.[130] With the correct choice of functional group in the corona, this technique could be used for many forms of decontamination, including biohazards and heavy metals.

Coronas with chemical responsiveness offer a route for sensing volatile organic compounds.[45,131] For example, Krasteva et al.[132] have fabricated dendrimer/gold nanoparticle sensors where the dendrimers swell in the presence of solvent vapors, changing the interparticle distances between the gold particles and thus the electrical conductivity of the films. This approach is readily extensible, as the correct choice of corona can allow for the sensing of a wide range of volatile compounds, since, as seen earlier, the various brush conformation models indicate that the size of the corona not only depends on the interaction parameter between the solvent and the corona, but also on the initial HNP design.[133] The effect is not limited to electrical conductivity—a particularly useful phenomenon is the effect of interparticle distance on the coupling of surface plasmon resonances between noble metal nanoparticles. Changes in coupling translate to changes in the color of the system, creating a "plasmon ruler" that can be calibrated to a resolution of less than 1 nm.[134]



https://doi.org/10.1557/mrc.2013.9 Published online by Cambridge University Press

Similarly, a gold nanorod-based fluid was shown to change color on shear due to a change in alignment of the rods; a confined layer could thus be used as a shear sensor.[135] The effect of the physical environment on the interparticle distance, and the concurrent effect on the film's electrical or optical properties can also be applied to create strain gauges[136,137] and temperature sensors.[138]

The modularity in the HNP design also implies that the nanoparticle core can provide a response to the environment when processability and stability necessitate a common corona design. Fabregat et al.[139] have shown that the fluorescent properties of thin films of polymers doped with quantum dots change with varying concentrations of nitrogen oxide compounds. Similar HNP systems might well be used for sensing other gases. While much of the work reported so far is focused on thin films deposited on hard patterned substrates, by exploiting the toughness created by entangled coronas, it should be possible to create robust freestanding sensors.

Another area in which neat HNP fluids offer an advantage over nanoparticle suspensions is their exceptionally stable dispersion. This is of particular interest in creating high-performance lubricants: nanoparticles can add wear resistance to a conventional lubricant.[140] The corona prevents the nanoparticles from agglomerating into grit, while the nanoparticles form a stable interfacial film between the two surfaces. While Archer and Kim specifically reported HNP systems that were added at up to 45% w/w in a base oil solvent, reports of extremely low friction seen between polymer brushes in a collapsed state suggest that HNPs without a solvent may also be extremely effective as lubricants.[141]

Voevodin et al.[142,143] were the first to study the lubricating properties of neat HNPs, in particular at the contact surfaces of the switches on microelectromechanical systems (MEMS). Previous attempts to lubricate MEMS switch contacts involved self-assembled monolayers of thiolates, but these were found to be thermally unstable. By using metallic (Au or Pt) nanoparticles and an ionically tethered low viscosity corona, surface roughness was increased, reducing contact area and thus reducing van der Waals force-mediated friction. Since the cores were metallic, they were able to dramatically improve the resistance of the switches to wear without compromising conductivity, increasing durability of the switch in the most extreme environments by over two orders of magnitude. In addition, the lubricant could flow into the contact areas, healing the protective film without external stimulus, again a major improvement on previous static protective layers (Fig. 6).

The combination of high inorganic fraction and the "self-healing" nature of fluids imply neat HNPs may be used for many other applications as well. High-energy capacitors, for example, require homogeneous films with high dielectric constants. The dielectric failure mode and thermo-mechanical properties of polymers, particularly their elasticity and toughness, are ideally suited for film processing of electrostatic capacitors that fail gracefully. However, their low dielectric constant limits the maximum energy storage density. Conversely, ceramics with high dielectric constants are brittle, difficult to process into complex shapes and exhibit catastrophic failure. HNP assemblies combine the best of both worlds by creating homogeneous, flexible materials with uniform nanoscale organization, with an inorganic content that can exceed 30% by volume. Initial studies on $TiO_2$/polystyrene HNP systems with high dielectric constants show that the concept is workable, but purity of the final material is critical to maintaining high breakdown fields.[74] For batteries and supercapacitors, ionically conductive electrolytes are desired. HNP-based electrolytes for lithium-ion batteries have higher mechanical strength than pure polymer electrolytes and exhibit superionic conductivities.[144] Their soft-glass nature makes them more flexible and easier to process than ceramic electrolytes, while the nanoparticles form a "maze" that restricts dendrite growth.[145] A similar concept could also be used to create magnetic films by using superparamagnetic nanoparticles (such

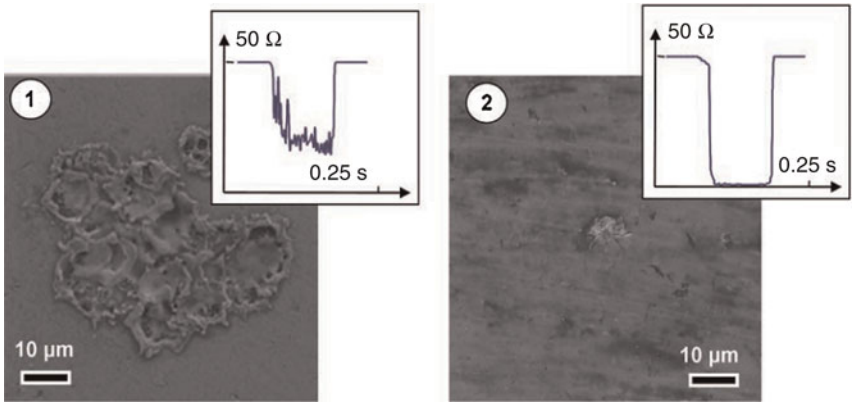



**Figure 6.** SEM images from Ref. 142 of an unmodified gold MEMS relay contact (left) and a gold HNP-coated contact (right) after $10^3$ cycles. The insets show the impedance for a single switching cycle—the HNP-coated contact has lower noise and lower impedance in the closed position. (Reproduced with permission, copyright 2007 John Wiley & Sons).


https://doi.org/10.1557/mrc.2013.9 Published online by Cambridge University Press

as $Fe_3O_4$). By preventing the particles from aggregating, their superparamagnetism is retained, while the softness of the HNP system makes it suitable for thin-film coatings in applications where Mu-metal and similar high-permeability alloys are too rigid. A conceptually similar application is the creation of flexible radiation shields by incorporating a high Z element as the nanoparticle.[146] For many of these applications, greater the inorganic content, greater the functionality, making neat HNP systems much more attractive than traditional polymer nanocomposites (PNCs).

The ability to create organized arrays of nanoparticles opens up a number of informational applications. Ohno and others grafted PMMA (MW = 158 kDa) on the surface of 130 nm nanoparticles, and found that as they increased the concentration of the suspension, they were able to form a photonic crystal that exhibited Bragg diffraction in the visible regime.[147] By varying the molecular weight of the grafted brush and the radius of the particle, and exploiting the degree of entanglement discussed above, it would be possible to create large freestanding arrays of nanoparticles exhibiting wavelength-selective responses to light. These hybrid photonic crystals would have a significant advantage over conventional micron-sized particle superlattice crystals in that they would retain the fracture resistance and processability of the polymer that makes up the brush. Following from the recent studies of the dielectric properties of $TiO_2$-PS HNPs,[74] optically transparent films that combine the processability of neat HNPs with high refractive index ($n > 3$) and low scattering loss (no morphological features less than 1/10th of the wavelength of incident light) are possible. New optical coatings and metamaterials with complex refractive index profiles would then be feasible for use as gradient refractive index (GRIN) lenses and fiber and slab lasing media. This could be further combined with the layer-by-layer procedure described above to create a photonic material that has a smoothly varying lattice constant through the material, forming a graded photonic material that can be utilized to bend light in complex paths.[148]

A related application is the creation of phononic materials. These acoustic metamaterials have a phonon bandgap analogous to the photon bandgap of photonic crystals, making them useful as filters for both sound and thermal energy.[149,150] Instead of modulating the refractive index, phononic crystals modulate the mechanical properties in the lattice. The density/stiffness contrast between the nanoparticles and the polymer make assemblies of inorganic/organic HNPs an intriguing platform for such materials.

Finally, applications can be expanded beyond direct integration of neat HNP assemblies; it is possible to utilize the highly controlled hybrid morphologies as processing templates or green bodies for conversion to other materials. A particularly novel example is the use of neat ordered HNP systems as a precursor material to create nanoporous thin films of carbon (used in catalytic supports and chromatographic packing), as reported by Tang et al.[151] After casting thin films of a neat HNP system consisting of silica particles grafted with a dense polyacrylonitrile brush, they carbonized the polyacrylonitrile in an $N_2$ atmosphere, and then etched away the silica to create a carbon film with well-spaced pores with a narrow size distribution (Fig. 7). Using HNPs as the template for the films allows the spacing (and therefore the areal density) of the pores to be controlled over a wide range. In contrast, a particle/polymer blend used as a template would exhibit aggregation once the particle density became too high, forcing a trade-off between maximum pore density, processability, shrinkage, and a tight pore size distribution. Thus, HNP processability in combination with additive processing and patterning techniques provide opportunities to improve complex green body manufacturing.

## Conclusions

In summary, neat HNPs are a unique class of hybrid materials and offer new opportunities for fundamental studies and technological exploitation. Their versatility is underlined by the variety of ways in which neat HNP-based materials can be viewed; as toughened assemblies of nanoparticles, as nanoparticle fluids with low vapor pressure, as building blocks for complex nanostructures, as polymeric materials with unique

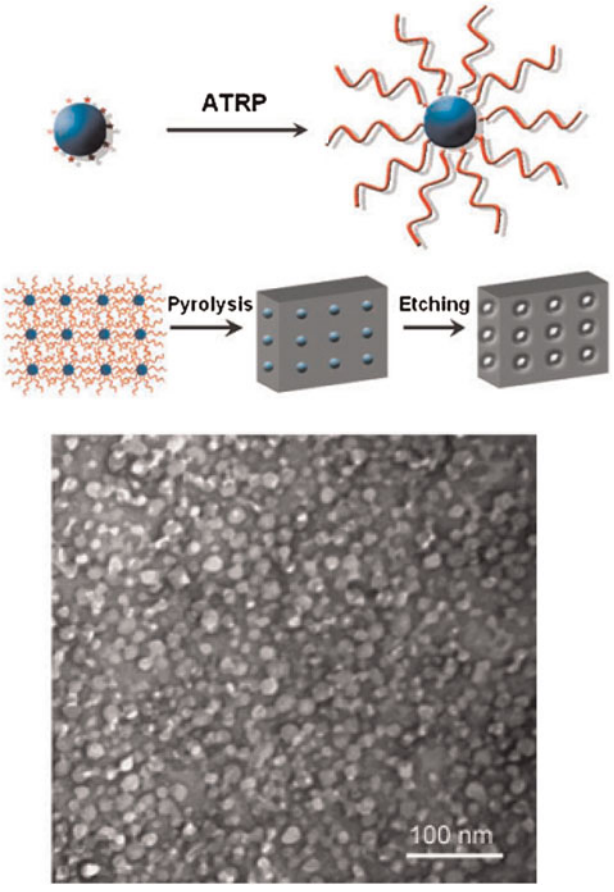



**Figure 7.** Schematic (above) and TEM (below) of nanoporous films produced from silica/polyacrylonitrile HNPs. (Reproduced with permission from Ref. 151, copyright 2008 John Wiley & Sons).



https://doi.org/10.1557/mrc.2013.9 Published online by Cambridge University Press

properties such as high polarizibility and magnetic permeability, as nanocomposites with stable processing-independent structures and properties, and, uniquely, as functional materials with capabilities that are beyond those of their components. While significant strides have been made, major hurdles remain to be overcome before there can be broad adoption of these materials as an applications platform. These hurdles include scale-up synthesis of large volumes while retaining purity, and a theoretical framework for a materials-by-design approach (which has only recently begun to emerge). Recent advances in polymer and nanoparticle synthesis and improved models for understanding the behavior of HNPs are on their way to addressing some of these challenges, thus paving the way for their widespread adoption.

## Acknowledgments

This publication is based on work supported in part by Award No. KUS-C1-018-02, made by King Abdullah University of Science and Technology (KAUST). This material is based upon work supported by the National Science Foundation under Grant No. IIP-1114275 and work supported by NYSERDA under Grant No. 18507. NYSERDA has not reviewed the information contained herein, and the opinions expressed in this report do not necessarily reflect those of NYSERDA or the State of New York. This work was funded in part by the Materials and Manufacturing Directorate of the Air Force Research Laboratory and the Air Force Office of Scientific Research.

## References

1. R. Mezzenga and J. Ruokolainen: Nanocomposites: nanoparticles in the right place. *Nat. Mater.* **8**, 926–928 (2009).
2. A.J. Crosby and J. Lee: Polymer nanocomposites: the 'nano' effect on mechanical properties. *Polym. Rev.* **47**, 217–229 (2007).
3. R. Krishnamoorti and R.A. Vaia: Polymer nanocomposites. *J. Polym. Sci. Part B: Polym. Phys.* **45**, 3252–3256 (2007).
4. S.K. Kumar and R. Krishnamoorti: Nanocomposites: structure, phase behavior, and properties. *Annu. Rev. Chem. Biomol. Eng.* **1**, 37–58 (2010).
5. K.I. Winey and R.A. Vaia: Polymer nanocomposites. *MRS Bull.* **32**, 314–322 (2007).
6. R.A. Vaia and J.F. Maguire: Polymer nanocomposites with prescribed morphology: going beyond nanoparticle-filled polymers. *Chem. Mater.* **19**, 2736–2751 (2007).
7. A.-S. Robbes, F. Cousin, F. Meneau, F. Dalmas, F. Boué, and J. Jestin: Nanocomposite materials with controlled anisotropic reinforcement triggered by magnetic self-assembly. *Macromolecules* **44**, 8858–8865 (2011).
8. M.E. Mackay, A. Tuteja, P.M. Duxbury, C.J. Hawker, B. Van Horn, Z. Guan, G. Chen, and R.S. Krishnan: General strategies for nanoparticle dispersion. *Science* **311**, 1740–1743 (2006).
9. M. van der Waarden: Stabilization of carbon-black dispersions in hydrocarbons. *J. Colloid Sci.* **5**, 317–325 (1950).
10. D.H. Napper. *Polymeric Stabilization of Colloidal Dispersions* (Academic Press, London, 1983).
11. T.A. Witten and P.A. Pincus: Colloid stabilization by long grafted polymers. *Macromolecules* **19**, 2509–2513 (1986).
12. R. Krishnamoorti: Strategies for dispersing nanoparticles in polymers. *MRS Bull.* **32**, 341–347 (2007).
13. S. Fischer, A. Salcher, A. Kornowski, H. Weller, and S. Förster: Completely miscible nanocomposites. *Angew. Chem. Int. Ed. Engl.* **50**, 7811–7814 (2011).
14. P. Akcora, H. Liu, S.K. Kumar, J. Moll, Y. Li, B.C. Benicewicz, L. S. Schadler, D. Acehan, A.Z. Panagiotopoulos, V. Pryamitsyn, V. Ganesan, J. Ilavsky, P. Thiyagarajan, R.H. Colby, and J.F. Douglas: Anisotropic self-assembly of spherical polymer-grafted nanoparticles. *Nat Mater* **8**, 354–359 (2009).
15. S. Coppée, S. Gabriele, A.M. Jonas, J. Jestin, and P. Damman: Influence of chain interdiffusion between immiscible polymers on dewetting dynamics. *Soft Matter* **7**, 9951 (2011).
16. IUPAC. Compendium of Chemical Terminology, 2nd ed. (the "Gold Book"). Compiled by A. D. McNaught and A. Wilkinson (Blackwell Scientific Publications, Oxford, 1997).
17. D. Vlassopoulos and G. Fytas: From Polymers to Colloids: Engineering the Dynamic Properties of Hairy Particles. In *Advances in Polymer Science: High Solid Dispersions*, edited by M. Cloitre (Springer, **236**, Berlin, Heidelberg, 2010), pp. 1–54.
18. C.N. Likos, H. Löwen, M. Watzlawek, B. Abbas, O. Jucknischke, J. Allgaier, and D. Richter: Star polymers viewed as ultrasoft colloidal particles. *Phys. Rev. Lett.* **80**, 4450–4453 (1998).
19. J. Gohy: Block Copolymer Micelles. In *Block Copolymers II*, edited by V. Abetz (Springer-Verlag, **190**, Berlin, 2005). pp. 65–136.
20. N. Osterman, D. Babic˘, I. Poberaj, J. Dobnikar, and P. Ziherl: Observation of condensed phases of quasiplanar core-softened colloids. *Phys. Rev.Lett.* **99**, 248301 (2007).
21. M. Daoud and J. Cotton: Star shaped polymers : a model for the conformation and its concentration dependence. *J. Phys.* **43**, 531–538 (1982).
22. D. Dukes, Y. Li, S. Lewis, B. Benicewicz, L. Schadler, and S.K. Kumar: Conformational transitions of spherical polymer brushes: synthesis, characterization, and theory. *Macromolecules* **43**, 1564–1570 (2010).
23. K. Ohno, T. Morinaga, S. Takeno, Y. Tsujii, and T. Fukuda: Suspensions of silica particles grafted with concentrated polymer brush: effects of graft chain length on brush layer thickness and colloidal crystallization. *Macromolecules* **40**, 9143–9150 (2007).
24. S.T. Milner, T.A. Witten, and M.E. Cates: Theory of the grafted polymer brush. *Macromolecules* **21**, 2610–2619 (1988).
25. C.M. Wijmans and E.B. Zhulina: Polymer brushes at curved surfaces. *Macromolecules* **26**, 7214–7224 (1993).
26. C.N. Likos: Effective interactions in soft condensed matter physics. *Phys. Rep.* **348**, 267–439 (2001).
27. M. Watzlawek, C.N. Likos, and H. Löwen: Phase diagram of star polymer solutions. *Phys. Rev. Lett.* **82**, 5289–5292 (1999).
28. J.U. Kim and M.W. Matsen: Interaction between polymer-grafted particles. *Macromolecules* **41**, 4435–4443 (2008).
29. V. Goel, J. Pietrasik, H. Dong, J. Sharma, K. Matyjaszewski, and R. Krishnamoorti: Structure of polymer tethered highly grafted nanoparticles. *Macromolecules* **44**, 8129–8135 (2011).
30. V. Goel, J. Pietrasik, K. Matyjaszewski, and R. Krishnamoorti: Linear viscoelasticity of spherical $SiO_2$ nanoparticle-tethered poly(butyl acrylate) hybrids. *Ind. Eng. Chem. Res.* **49**, 11985–11990 (2010).
31. H.-Y. Yu and D.L. Koch: Structure of solvent-free nanoparticle-organic hybrid materials. *Langmuir* **26**, 16801–16811 (2010).
32. A. Chremos, A.Z. Panagiotopoulos, H.-Y. Yu, and D.L. Koch: Structure of solvent-free grafted nanoparticles: molecular dynamics and density-functional theory. *J. Chem. Phys.* **135**, 114901 (2011).
33. B. Hong, A. Chremos, and A.Z. Panagiotopoulos: Dynamics in coarse-grained models for oligomer-grafted silica nanoparticles. *J. Chem. Phys.* **136**, 204904 (2012).
34. A. Chremos and A. Panagiotopoulos: Structural transitions of solvent-free oligomer-grafted nanoparticles. *Phys. Rev. Lett.* **107**, 105503 (2011).
35. K.J.M. Bishop, C.E. Wilmer, S. Soh, and B.A. Grzybowski: Nanoscale forces and their uses in self-assembly. *Small* **5**, 1600–1630 (2009).
36. P. Akcora, S.K. Kumar, V. Garci'a Sakai, Y. Li, B.C. Benicewicz, and L. S. Schadler: Segmental dynamics in PMMA-grafted nanoparticle composites. *Macromolecules* **43**, 8275–8281 (2010).
37. P. Akcora, S.K. Kumar, J. Moll, S. Lewis, L.S. Schadler, Y. Li, B. C. Benicewicz, A. Sandy, S. Narayanan, J. Ilavsky, P. Thiyagarajan, R.


https://doi.org/10.1557/mrc.2013.9 Published online by Cambridge University Press

H. Colby, and J.F. Douglas: 'Gel-like' mechanical reinforcement in polymer nanocomposite melts. *Macromolecules* **43**, 1003–1010 (2010).
38. M.E. McEwan, S.a. Egorov, J. Ilavsky, D.L. Green, and Y. Yang: Mechanical reinforcement of polymer nanocomposites: theory and ultra-small angle x-ray scattering (USAXS) studies. *Soft Matter* **7**, 2725 (2011).
39. J. Choi, C.M. Hui, J. Pietrasik, H. Dong, K. Matyjaszewski, and M. R. Bockstaller: Toughening fragile matter: mechanical properties of particle solids assembled from polymer-grafted hybrid particles synthesized by ATRP. *Soft Matter* **8**, 4072 (2012).
40. P. Agarwal, M. Chopra, and L.A. Archer: Nanoparticle netpoints for shape-memory polymers. *Angew. Chem. Int. Ed. Engl.* **50**, 8670–8673 (2011).
41. B.V.S. Iyer, I.G. Salib, V.V. Yashin, T. Kowalewski, K. Matyjaszewski, and A.C. Balazs: Modeling the response of dual cross-linked nanoparticle networks to mechanical deformation. *Soft Matter* **9**, 109–121 (2013). doi:10.1039/c2sm27121d
42. S. Torquato, S. Hyun, and A. Donev: Multifunctional composites: optimizing microstructures for simultaneous transport of heat and electricity. *Phys. Rev. Lett.* **89**, 266601 (2002).
43. J.K. Guest and J.H. Prévost: Optimizing multifunctional materials: design of microstructures for maximized stiffness and fluid permeability. *Int. J. Solids Struct.* **43**, 7028–7047 (2006).
44. K. Hur, R.G. Hennig, F.A. Escobedo, and U. Wiesner: Mesoscopic structure prediction of nanoparticle assembly and coassembly: theoretical foundation. *J. Chem. Phys.* **133**, 194108 (2010).
45. R. Shenhar, T.B. Norsten, and V.M. Rotello: Polymer-mediated nanoparticle assembly: structural control and applications. *Adv. Mater.* **17**, 657–669 (2005).
46. C.-T. Lo, B. Lee, N.L.D. Rago, R.E. Winans, and P. Thiyagarajan: Strategy for better ordering in diblock copolymer based nanocomposites. *Macromol. Rapid Commun.* **28**, 1607–1612 (2007).
47. M.R. Bockstaller, R.A. Mickiewicz, and E.L. Thomas: Block copolymer nanocomposites: perspectives for tailored functional materials. *Adv. Mater.* **17**, 1331–1349 (2005).
48. X. Zhu, L. Wang, J. Lin, and L. Zhang: Ordered nanostructures self-assembled from block copolymer tethered nanoparticles. *ACS Nano* **4**, 4979–4988 (2010).
49. G.-K. Xu, X.-Q. Feng, and S.-W. Yu: Controllable nanostructural transitions in grafted nanoparticle-block copolymer composites. *Nano Res.* **3**, 356–362 (2010).
50. M. Wojcik, W. Lewandowski, J. Matraszek, J. Mieczkowski, J. Borysiuk, D. Pociecha, and E. Gorecka: Liquid-crystalline phases made of gold nanoparticles. *Angew. Chem. Int. Ed. Engl.* **48**, 5167–5169 (2009).
51. I. In, Y. Jun, Y.J. Kim, and S.Y. Kim: Spontaneous one dimensional arrangement of spherical Au nanoparticles with liquid crystal ligands. *Chem. Commun. (Camb.)* (6), 800–801 (2005). doi:10.1039/b413510e
52. J. He, Y. Liu, T. Babu, Z. Wei, and Z. Nie: Self-assembly of inorganic nanoparticle vesicles and tubules driven by tethered linear block copolymers. *J. Am. Chem. Soc.* **134**, 11342–11345 (2012).
53. Y. Guo, S. Harirchian-Saei, C.M.S. Izumi, and M.G. Moffitt: Block copolymer mimetic self-assembly of inorganic nanoparticles. *ACS Nano* **5**, 3309–3318 (2011).
54. A. Jayaraman and K.S. Schweizer: Effective interactions and self-assembly of hybrid polymer grafted nanoparticles in a homopolymer matrix. *Macromolecules* **42**, 8423–8434 (2009).
55. A. Jayaraman and K.S. Schweizer: Structure and assembly of dense solutions and melts of single tethered nanoparticles. *J. Chem. Phys.* **128**, 164904 (2008).
56. A. Jayaraman and K.S. Schweizer: Effect of the number and placement of polymer tethers on the structure of concentrated solutions and melts of hybrid nanoparticles. *Langmuir* **24**, 11119–11130 (2008).
57. C.R. Iacovella and S.C. Glotzer: Complex crystal structures formed by the self-assembly of ditethered nanospheres. *Nano Lett.* **9**, 1206–1211 (2009).
58. C.L. Phillips, C.R. Iacovella, and S.C. Glotzer: Stability of the double gyroid phase to nanoparticle polydispersity in polymer-tethered nanosphere systems. *Soft Matter* **6**, 1693 (2010).
59. B. Wang, B. Li, B. Dong, B. Zhao, and C.Y. Li: Homo- and hetero-particle clusters formed by Janus nanoparticles with bicompartment polymer brushes. *Macromolecules* **43**, 9234–9238 (2010).
60. Y. Xia, Y. Xiong, B. Lim, and S.E. Skrabalak: Shape-controlled synthesis of metal nanocrystals: simple chemistry meets complex physics? *Angew. Chem. Int. Ed. Engl.* **48**, 60–103 (2009).
61. A. Guerrero-Martínez, S. Barbosa, I. Pastoriza-Santos, and L. M. Liz-Marzán: Nanostars shine bright for you. *Curr. Opin. Colloid Interface Sci.* **16**, 118–127 (2011).
62. C. Wang, C. Xu, H. Zeng, and S. Sun: Recent progress in syntheses and applications of dumbbell-like nanoparticles. *Adv. Mater. Weinheim* **21**, 3045–3052 (2009).
63. S.C. Glotzer, M.A. Horsch, C.R. Iacovella, Z. Zhang, E.R. Chan, and X. Zhang: Self-assembly of anisotropic tethered nanoparticle shape amphiphiles. *Curr. Opin. Colloid Interface Sci.* **10**, 287–295 (2005).
64. M.A. Horsch, M.H. Lamm, and S.C. Glotzer: Tethered nano building blocks: toward a conceptual framework for nanoparticle self-assembly. *Nano Lett.* **3**, 1341–1346 (2003).
65. S.C. Glotzer and M.J. Solomon: Anisotropy of building blocks and their assembly into complex structures. *Nat. Mater.* **6**, 557–562 (2007).
66. D. Nykypanchuk, M.M. Maye, D. van der Lelie, and O. Gang: DNA-guided crystallization of colloidal nanoparticles. *Nature* **451**, 549–552 (2008).
67. J.M. Slocik, F. Tam, N.J. Halas, and R.R. Naik: Peptide-assembled optically responsive nanoparticle complexes. *Nano Lett.* **7**, 1054–1058 (2007).
68. S.C. Glotzer: Self-assembly of patchy particles. *Nano Lett.* **4**, 1407–1413 (2004).
69. G. Malescio and G. Pellicane: Stripe phases from isotropic repulsive interactions. *Nat. Mater.* **2**, 97–100 (2003).
70. C.N. Likos: Soft matter with soft particles. *Soft Matter* **2**, 478 (2006).
71. A.K. Kandar, S. Srivastava, J.K. Basu, M.K. Mukhopadhyay, S. Seifert, and S. Narayanan: Unusual dynamical arrest in polymer grafted nanoparticles. *J. Chem. Phys.* **130**, 121102 (2009).
72. P. Agarwal, S. Srivastava, and L. Archer: Thermal jamming of a colloidal glass. *Phys. Rev. Lett.* **107**, 268302 (2011).
73. D.A. Savin, J. Pyun, G.D. Patterson, T. Kowalewski, and K. Matyjaszewski: Synthesis and characterization of silica-graft-polystyrene hybrid nanoparticles: effect of constraint on the glass-transition temperature of spherical polymer brushes. *J. Polym. Sci. Part B: Polym. Phys.* **40**, 2667–2676 (2002).
74. M.N. Tchoul, S.P. Fillery, H. Koerner, L.F. Drummy, F.T. Oyerokun, P. A. Mirau, M.F. Durstock, and R.A. Vaia: Assemblies of titanium dioxide-polystyrene hybrid nanoparticles for dielectric applications. *Chem. Mater.* **22**, 1749–1759 (2010).
75. P. Agarwal, H. Qi, and L.A. Archer: The ages in a self-suspended nanoparticle liquid. *Nano Lett.* **10**, 111–115 (2010).
76. R. Rodriguez, R. Herrera, L.A. Archer, and E.P. Giannelis: Nanoscale ionic materials. *Adv. Mater.* **20**, 4353–4358 (2008).
77. A.B. Bourlinos, R. Herrera, N. Chalkias, D.D. Jiang, Q. Zhang, L. A. Archer, and E.P. Giannelis: Surface-functionalized nanoparticles with liquid-like behavior. *Adv. Mater.* **17**, 234–237 (2005).
78. D.S. Pearson and E. Helfand: Viscoelastic properties of star-shaped polymers. *Macromolecules* **17**, 888–895 (1984).
79. A. Chremos, A.Z. Panagiotopoulos, and D.L. Koch: Dynamics of solvent-free grafted nanoparticles. *J. Chem. Phys.* **136**, 044902 (2012).
80. A.B. Bourlinos, E.P. Giannelis, Q. Zhang, L.A. Archer, G. Floudas, and G. Fytas: Surface-functionalized nanoparticles with liquid-like behavior: the role of the constituent components. *Eur. Phys. J. E Soft Matter* **20**, 109–117 (2006).
81. A.B. Bourlinos, S. Ray Chowdhury, R. Herrera, D.D. Jiang, Q. Zhang, L. A. Archer, and E.P. Giannelis: Functionalized nanostructures with liquid-like behavior: expanding the gallery of available nanostructures. *Adv. Funct. Mater.* **15**, 1285–1290 (2005).
82. R. Rodriguez, R. Herrera, A.B. Bourlinos, R. Li, A. Amassian, L. A. Archer, and E.P. Giannelis: The synthesis and properties of nanoscale ionic materials. *Appl. Organometal. Chemis.* **24**, 581–589 (2010).
83. B. Hong, A. Chremos, and A.Z. Panagiotopoulos: Simulations of the structure and dynamics of nanoparticle-based ionic liquids. *Faraday Discus.* **154**, 29 (2012).



https://doi.org/10.1557/mrc.2013.9 Published online by Cambridge University Press

84. M.L. Jespersen, P.A. Mirau, E. von Meerwall, R.A. Vaia, R. Rodriguez, and E.P. Giannelis: Canopy dynamics in nanoscale ionic materials. *ACS Nano* **4**, 3735–3742 (2010).
85. H. Cui, Y. Feng, W. Ren, T. Zeng, H. Lv, and Y. Pan: Strategies of large scale synthesis of monodisperse nanoparticles. *Recent Pat. Nanotechnol.* **3**, 32–41 (2009).
86. O. Masala and R. Seshadri: Synthesis routes for large volumes of nanoparticles. *Annu. Rev. Mater. Res.* **34**, 41–81 (2004).
87. G. Liu, X. Yan, Z. Lu, S.a. Curda, and J. Lal: One-pot synthesis of block copolymer coated cobalt nanocrystals. *Chem. Mater.* **17**, 4985–4991 (2005).
88. Y. Zhang, S. Luo, and S. Liu: Fabrication of hybrid nanoparticles with thermoresponsive coronas via a self-assembling approach. *Macromolecules* **38**, 9813–9820 (2005).
89. R. Subbiah, M. Veerapandian, and K.S. Yun: Nanoparticles: functionalization and multifunctional applications in biomedical sciences. *Curr. Med. Chem.* **17**, 4559–4577 (2010).
90. M.-A. Neouze and U. Schubert: Surface modification and functionalization of metal and metal oxide nanoparticles by organic ligands. *Monatshefte Chem. – Chem. Monthly* **139**, 183–195 (2008).
91. R.B. Grubbs: Roles of polymer ligands in nanoparticle stabilization. *Polym. Rev.* **47**, 197–215 (2007).
92. W.P. Wuelfing, S.M. Gross, D.T. Miles, and R.W. Murray: Nanometer gold clusters protected by surface-bound monolayers of thiolated poly (ethylene glycol) polymer electrolyte. *J. Am. Chem. Soc.* **120**, 12696–12697 (1998).
93. M.K. Corbierre, N.S. Cameron, and R.B. Lennox: Polymer-stabilized gold nanoparticles with high grafting densities. *Langmuir* **20**, 2867–2873 (2004).
94. Y. Zheng, J. Zhang, L. Lan, P. Yu, R. Rodriguez, R. Herrera, D. Wang, and E.P. Giannelis: Preparation of solvent-free gold nanofluids with facile self-assembly technique. *Chemphyschem* **11**, 61–64 (2010).
95. S. Mehdizadeh Taheri, S. Fischer, and S. Förster: Routes to nanoparticle-polymer superlattices. *Polymers* **3**, 662–673 (2011).
96. L.S. Penn, H. Huang, M.D. Sindkhedkar, S.E. Rankin, K. Chittenden, R. P. Quirk, R.T. Mathers, and Y. Lee: Formation of tethered nanolayers: three regimes of kinetics. *Macromolecules* **35**, 7054–7066 (2002).
97. F.T. Oyerokun and R.A. Vaia: Distribution in the grafting density of end-functionalized polymer chains adsorbed onto nanoparticle surfaces. *Macromolecules* **45**, 7649–7659 (2012).
98. E. Hübner, J. Allgaier, M. Meyer, J. Stellbrink, W. Pyckhout-Hintzen, and D. Richter: Synthesis of polymer/silica hybrid nanoparticles using anionic polymerization techniques. *Macromolecules* **43**, 856–867 (2010).
99. B.L. Papke, L.S. Bartley, and C.A. Migdal: Adsorption of poly(isobutenyl) succinimide dispersants onto calcium alkylarylsulfonate colloidal dispersions in hydrocarbon media. *Langmuir* **7**, 2614–2619 (1991).
100. N. Fernandes, P. Dallas, R. Rodriguez, A.B. Bourlinos, V. Georgakilas, and E.P. Giannelis: Fullerol ionic fluids. *Nanoscale* **2**, 1653–1656 (2010).
101. N.J. Fernandes, J. Akbarzadeh, H. Peterlik, and E.P. Giannelis: Synthesis and properties of highly dispersed ionic silica-poly(ethylene oxide) nanohybrids. *ACS Nano* **7**, 1265–1271 (2013). doi:10.1021/nn304735r
102. B. Radhakrishnan, R. Ranjan, and W.J. Brittain: Surface initiated polymerizations from silica nanoparticles. *Soft Matter* **2**, 386 (2006).
103. R.C. Advincula: Surface initiated polymerization from nanoparticle surfaces. *J. Dispers. Sci. Technol.* **24**, 343–361 (2003).
104. J. Pyun and K. Matyjaszewski: Synthesis of nanocomposite organic/inorganic hybrid materials using controlled/'living' radical polymerization. *Chem. Mater.* **13**, 3436–3448 (2001).
105. Q. Zhou, S. Wang, X. Fan, R. Advincula, and J. Mays: Living anionic surface-initiated polymerization (LASIP) of a polymer on silica nanoparticles. *Langmuir* **18**, 3324–3331 (2002).
106. R. Jordan, N. West, A. Ulman, Y.-M. Chou, and O. Nuyken: Nanocomposites by surface-initiated living cationic polymerization of 2-oxazolines on functionalized gold nanoparticles. *Macromolecules* **34**, 1606–1611 (2001).
107. K. Min, H. Gao, J.A. Yoon, W. Wu, T. Kowalewski, and K. Matyjaszewski: One-pot synthesis of hairy nanoparticles by emulsion ATRP. *Macromolecules* **42**, 1597–1603 (2009).
108. K. Matyjaszewski, H. Dong, W. Jakubowski, J. Pietrasik, and A. Kusumo: Grafting from surfaces for 'everyone': ARGET ATRP in the presence of air. *Langmuir* **23**, 4528–4531 (2007).
109. K. Matyjaszewski and N.V. Tsarevsky: Nanostructured functional materials prepared by atom transfer radical polymerization. *Nat. Chem.* **1**, 276–288 (2009).
110. M.H. Stenzel: Hairy Core-Shell Nanoparticles via RAFT: where are the opportunities and where are the problems and challenges?. *Macromol. Rapid Commun.* **30**, 1603–1624 (2009).
111. C. Li and B.C. Benicewicz: Synthesis of well-defined polymer brushes grafted onto silica nanoparticles via surface reversible addition – fragmentation chain transfer polymerization. *Macromolecules* **38**, 5929–5936 (2005).
112. Y. Li and B.C. Benicewicz: Functionalization of silica nanoparticles via the combination of surface-initiated raft polymerization and click reactions. *Macromolecules* **41**, 7986–7992 (2008).
113. D.J. Siegwart, K.A. Whitehead, L. Nuhn, G. Sahay, H. Cheng, S. Jiang, M. Ma, A. Lytton-Jean, A. Vegas, P. Fenton, C.G. Levins, K.T. Love, H. Lee, C. Cortez, S.P. Collins, Y.F. Li, J. Jang, W. Querbes, C. Zurenko, T. Novobrantseva, R. Langer, and D.G. Anderson: Combinatorial synthesis of chemically diverse core-shell nanoparticles for intracellular delivery. *Proc. Natl. Acad. Sci. USA* **108**, 12996–13001 (2011).
114. C. Sanchez, B. Julián, P. Belleville, and M. Popall: Applications of hybrid organic–inorganic nanocomposites. *J. Mater. Chem.* **15**, 3559 (2005).
115. M. Trikeriotis, W.J. Bae, E. Schwartz, M. Krysak, N. Lafferty, P. Xie, B. Smith, P.A. Zimmerman, C.K. Ober, and E.P. Giannelis: Development of an inorganic photoresist for DUV, EUV, and electron beam imaging. In *Proceedings of SPIE*, M.L. Rieger, J. Thiele ed, 76390E-76390E-10 (Society of Photo-Optical Instrumentation Engineers DO - 10.1117/12.846672, 2010), pp. 7639.
116. N.A. Kotov: Ordered layered assemblies of nanoparticles. *MRS Bull.* **26**, 992–997 (2001).
117. Y. Kim, D. Kim, I. Kwon, H.W. Jung, and J. Cho: Solvent-free nanoparticle fluids with highly collective functionalities for layer-by-layer assembly. *J. Mater. Chem.* **22**, 11488 (2012).
118. J. Zhang, Q. Li, X. Di, Z. Liu, and G. Xu: Layer-by-layer assembly of multicolored semiconductor quantum dots towards efficient blue, green, red and full color optical films. *Nanotechnology* **19**, 435606 (2008).
119. N. Sakai, G.K. Prasad, Y. Ebina, K. Takada, and T. Sasaki: Layer-by-layer assembled $TiO_2$ nanoparticle/PEDOT-PSS composite films for switching of electric conductivity in response to ultraviolet and visible light. *Chem. Mater.* **18**, 3596–3598 (2006).
120. M.S. Mauter, Y. Wang, K.C. Okemgbo, C.O. Osuji, E.P. Giannelis, and M. Elimelech: Antifouling ultrafiltration membranes via post-fabrication grafting of biocidal nanomaterials. *ACS Appl. Mater. Interfaces* **3**, 2861–2868 (2011).
121. A. Tiraferri, Y. Kang, E.P. Giannelis, and M. Elimelech: Superhydrophilic thin-film composite forward osmosis membranes for organic fouling control: fouling behavior and antifouling mechanisms. *Environ. Sci. Technol.* **46**, 11135–11144 (2012).
122. A. Tiraferri, Y. Kang, E.P. Giannelis, and M. Elimelech: Highly hydrophilic thin-film composite forward osmosis membranes functionalized with surface-tailored nanoparticles. *ACS Appl. Mater. Interfaces* **4**, 5044–5053 (2012).
123. J. Fang, A. Kelarakis, L. Estevez, Y. Wang, R. Rodriguez, and E. P. Giannelis: Superhydrophilic and solvent resistant coatings on polypropylene fabrics by a simple deposition process. *J. Mater. Chem.* **20**, 1651 (2010).
124. D.M. Guldi, I. Zilbermann, G. Anderson, N.A. Kotov, N. Tagmatarchis, and M. Prato: Nanosized inorganic/organic composites for solar energy conversion. *J. Mater. Chem.* **15**, 114 (2005).
125. J.A. Labastide, M. Baghgar, I. Dujovne, Y. Yang, A.D. Dinsmore, B. G. Sumpter, D. Venkataraman, and M.D. Barnes: Polymer nanoparticle superlattices for organic photovoltaic applications. *J. Phys. Chem. Lett.* **2**, 3085–3091 (2011).
126. D.Y. Lee, J.T. Pham, J. Lawrence, C.H. Lee, C. Parkos, T. Emrick, and A. J. Crosby: Macroscopic nanoparticle ribbons and fabrics. *Adv. Mater. Weinheim* (2012). doi:10.1002/adma.201203719




https://doi.org/10.1557/mrc.2013.9 Published online by Cambridge University Press

127. H.S. Kim, C.H. Lee, P.K. Sudeep, T. Emrick, and A.J. Crosby: Nanoparticle stripes, grids, and ribbons produced by flow coating. *Adv. Mater. Weinheim* **22**, 4600–4604 (2010).
128. K.-Y.A. Lin and A.-H.A. Park: Effects of bonding types and functional groups on $CO_2$ capture using novel multiphase systems of liquid-like nanoparticle organic hybrid materials. *Environ. Sci. Technol.* **45**, 6633–6639 (2011).
129. Y. Park, J. Decatur, K.-Y.A. Lin, and A.-H.A. Park: Investigation of $CO_2$ capture mechanisms of liquid-like nanoparticle organic hybrid materials via structural characterization. *Phys. Chem. Chem. Phys.* **13**, 18115–18122 (2011).
130. P. Calcagnile, D. Fragouli, I.S. Bayer, G.C. Anyfantis, L. Martiradonna, P. D. Cozzoli, R. Cingolani, and A. Athanassiou: Magnetically driven floating foams for the removal of oil contaminants from water. *ACS Nano* **6**, 5413–5419 (2012).
131. A.N. Shipway, E. Katz, and I. Willner: Nanoparticle arrays on surfaces for electronic, optical, and sensor applications. *Chem. Phys. Chem.* **1**, 18–52 (2000).
132. N. Krasteva, I. Besnard, B. Guse, R.E. Bauer, K. Müllen, A. Yasuda, and T. Vossmeyer: Self-assembled gold nanoparticle/dendrimer composite films for vapor sensing applications. *Nano Lett.* **2**, 551–555 (2002).
133. L. Wang, X. Shi, N.N. Kariuki, M. Schadt, G.R. Wang, Q. Rendeng, J. Choi, J. Luo, S. Lu, and C.-J. Zhong: Array of molecularly mediated thin film assemblies of nanoparticles: correlation of vapor sensing with interparticle spatial properties. *J. Am. Chem. Soc.* **129**, 2161–2170 (2007).
134. C. Sönnichsen, B.M. Reinhard, J. Liphardt, and A.P. Alivisatos: A molecular ruler based on plasmon coupling of single gold and silver nanoparticles. *Nat. Biotechnol.* **23**, 741–745 (2005).
135. R.R. Bhattacharjee, R. Li, L. Estevez, D.-M. Smilgies, A. Amassian, and E.P. Giannelis: A plasmonic fluid with dynamically tunable optical properties. *J. Mater. Chem.* **19**, 8728 (2009).
136. T. Vossmeyer, C. Stolte, M. Ijeh, A. Kornowski, and H. Weller: Networked gold-nanoparticle coatings on polyethylene: charge transport and strain sensitivity. *Adv. Funct. Mater.* **18**, 1611–1616 (2008).
137. K.J. Loh and D. Chang: Zinc oxide nanoparticle-polymeric thin films for dynamic strain sensing. *J. Mater. Sci.* **46**, 228–237 (2010).
138. Y. Lu, G.L. Liu, and L.P. Lee: High-density silver nanoparticle film with temperature-controllable interparticle spacing for a tunable surface enhanced raman scattering substrate. *Nano Lett.* **5**, 5–9 (2005).
139. V. Fabregat, M.A. Izquierdo, M.I. Burguete, F. Galindo, and S.V. Luis: Quantum dot–polymethacrylate composites for the analysis of NOx by fluorescence spectroscopy. *Inorg. Chim. Acta* **381**, 212–217 (2012).
140. D. Kim and L.A. Archer: Nanoscale organic-inorganic hybrid lubricants. *Langmuir* **27**, 3083–3094 (2011).
141. A. Nomura, K. Okayasu, K. Ohno, T. Fukuda, and Y. Tsujii: Lubrication mechanism of concentrated polymer brushes in solvents: effect of solvent quality and thereby swelling state. *Macromolecules* **44**, 5013–5019 (2011).
142. A.A. Voevodin, R.A. Vaia, S.T. Patton, S. Diamanti, M. Pender, M. Yoonessi, J. Brubaker, J.-J. Hu, J.H. Sanders, B.S. Phillips, and R. I. MacCuspie: Nanoparticle-wetted surfaces for relays and energy transmission contacts. *Small* **3**, 1957–1963 (2007).
143. S.T. Patton, A.A. Voevodin, R.A. Vaia, M. Pender, S.J. Diamanti, and B. Phillips: Nanoparticle liquids for surface modification and lubrication of MEMS switch contacts. *J. Microelectromech. Syst.* **17**, 741–746 (2008).
144. J.L. Nugent, S.S. Moganty, and L.A. Archer: Nanoscale organic hybrid electrolytes. *Adv. Mater. Weinheim* **22**, 3677–3680 (2010).
145. S.S. Moganty, N. Jayaprakash, J.L. Nugent, J. Shen, and L.A. Archer: Ionic-liquid-tethered nanoparticles: hybrid electrolytes. *Angew. Chem.* **122**, 9344–9347 (2010).
146. S. Nambiar and J.T.W. Yeow: Polymer-composite materials for radiation protection. *ACS Appl. Mater. Interfaces* **4**, 5717–5726 (2012).
147. K. Ohno, T. Morinaga, S. Takeno, Y. Tsujii, and T. Fukuda: Suspensions of silica particles grafted with concentrated polymer brush: a new family of colloidal crystals. *Macromolecules* **39**, 1245–1249 (2006).
148. E. Centeno and D. Cassagne: Graded photonic crystals. *Opt. Lett.* **30**, 2278–2280 (2005).
149. W. Cheng, J. Wang, U. Jonas, G. Fytas, and N. Stefanou: Observation and tuning of hypersonic bandgaps in colloidal crystals. *Nat. Mater.* **5**, 830–836 (2006).
150. R.S. Penciu, H. Kriegs, G. Petekidis, G. Fytas, and E.N. Economou: Phonons in colloidal systems. *J. Chem. Phys.* **118**, 5224 (2003).
151. C. Tang, L. Bombalski, M. Kruk, M. Jaroniec, K. Matyjaszewski, and T. Kowalewski: Nanoporous carbon films from 'hairy' polyacrylonitrile-grafted colloidal silica nanoparticles. *Adv. Mater.* **20**, 1516–1522 (2008).




https://doi.org/10.1557/mrc.2013.9 Published online by Cambridge University Press